ANKARA YILDIRIM BEYAZIT UNIVERSITY

GRADUATE SCHOOL OF NATURAL AND APPLIED SCIENCES

EFFECT OF ADDITION WITH EPOXY POLYMER TO Sn-Bi SOLDER PASTE

M.Sc. Thesis by

Bülent ÖZCAN

Department of Materials Engineering

July, 2024

ANKARA

EFFECT OF ADDITION WITH EPOXY POLYMER TO Sn-Bi SOLDER PASTE

A Thesis Submitted to

The Graduate School of Natural and Applied Sciences of

Ankara Yıldırım Beyazıt University

In Partial Fulfillment of the Requirements for the Degree of Master of Science

in Materials Engineering, Department of Materials Engineering

by

Bülent ÖZCAN

July, 2024

ANKARA

M.Sc. THESIS EXAMINATION RESULT FORM

We have read the thesis entitled **“EFFECT OF ADDITION WITH EPOXY POLYMER TO Sn-Bi SOLDER PASTE”** completed by **Bülent ÖZCAN** under the supervision of **Prof. Dr. Güven ÇANKAYA** and we certify that in our opinion it is fully adequate, in scope and in quality, as a thesis for the degree of Master of Science.

Prof. Dr. Güven ÇANKAYA

Supervisor

Asst. Prof. İdris Tuğrul GÜLENÇ

Jury Member

Prof. Dr. Ahmet DURGUTLU

Jury Member

Prof. Dr. Sadettin ORHAN

Director

Graduate School of Natural and Applied Sciences

ETHICAL DECLARATION

I hereby declare that, in this thesis which has been prepared in accordance with the Thesis Writing Manual of Graduate School of Natural and Applied Sciences,

- All data, information and documents are obtained in the framework of academic and ethical rules,
- All information, documents and assessments are presented in accordance with scientific ethics and morals,
- All the materials that have been utilized are fully cited and referenced,
- No change has been made on the utilized materials,
- All the works presented are original,

and in any contrary case of above statements, I accept to renounce all my legal rights.

Date: 23.07.2024 **Signature: ………………………….**

Name & Surname: Bülent ÖZCAN

ACKNOWLEDGMENTS

My supervisor, Prof. Dr. Güven ÇANKAYA, is greatly appreciated for his invaluable guidance, advice, and support in making this project possible. From the start of this project to its completion, him for sharing his knowledge and skills with me, and I am grateful for that. Working with him has been a pleasure for me.

I would like to thank Research Assistant Semih AĞCA for the SEM measurements and for his help.

I would like to thank my family, who has been my biggest source of motivation for supporting and encouraging me throughout my life.

July, 2024 **Bülent ÖZCAN**

EFFECT OF ADDITION WITH EPOXY POLYMER TO Sn-Bi SOLDER PASTE

ABSTRACT

Eutectic tin-bismuth (58Bi42Sn) alloy is commonly used in low-temperature soldering because of its low melting temperatures, superior wettability, and low thermal expansion coefficients. The structure created using Sn-Bi solder paste has low strength due to the brittleness of the Bi phase, which prevents a good solder connection. This circumstance limits the applications of Sn-Bi solder paste. To overcome this disadvantage, a new solder paste was created by combining epoxy resin with Sn-Bi solder paste. We got the reflow profile by evaluating the melting parameters of the solder paste and the epoxy system's hardening reaction using differential scanning calorimetry (DSC). By these means, the solder paste was soldered at the optimal temperature. This new solder paste was tested for contact angle, spreading area, and drop test. The findings revealed that when the epoxy resin content was optimal, the mechanical characteristics of the solder improved, and a considerable improvement in the spreading area was observed with a higher contact angle when compared to Sn-Bi solder paste. In the study, it was observed that the solder made with epoxy addition was much more durable than normal solder in drop tests. The solder with 5 wt.% content, which we consider ideal, performed 2.6 times better than the epoxy-free solder. For this reason, the use of epoxy-added solders in vehicles sent to space or structures that will be exposed to high vibration will provide a significant advantage in terms of solder strength. In addition, covering the exterior surface of Sn-Bi solder paste with epoxy polymer provides a protective layer against external influences. Epoxy's ability to stick to diverse surfaces allows solder paste to be soldered on a variety of surfaces.

Keywords: Sn-Bi solder paste, epoxy resin, contact angle, spreading area

Sn-Bi LEHIM PASTASINA EPOKSİ POLİMER İLAVESİNİN ETKİSİ

ÖZ

Ötektik kalay-bizmut (58Bi42Sn) alaşımı, düşük erime sıcaklıkları, iyi ıslanabilirliği ve düşük termal genleşme katsayıları nedeniyle düşük sıcaklıkta lehimlemede yaygın olarak kullanılmaktadır. Sn-Bi lehim pastası ile elde edilen yapı, iyi bir lehim bağlantısı sağlamayan Bi fazının kırılganlığından dolayı düşük mukavemete sahiptir. Bu durum Sn-Bi lehim pastasının kullanım alanlarını sınırlamaktadır. Bu çalışmada bu dezavantajı ortadan kaldırmak amacıyla Sn-Bi lehim pastasına epoksi reçine ilave edilerek yeni bir lehim pastası elde edilmiştir. Bu lehim pastasının erime özelliklerini ve epoksi sisteminin sertleşme reaksiyonunu diferansiyel tarama kalorimetrisi (DSC) ile ölçerek yeniden akış profilini elde ettik. Bu sayede lehim pastasının optimum sıcaklıklar kullanılarak lehimlenmesi sağlandı. Bu yeni lehim pastası temas açısı, yayılma alanı ve düşme testlerine tabi tutuldu. Sonuçlar, epoksi reçine içeriği optimum aralıkta olduğunda lehimin mekanik özelliklerinin daha iyi olduğunu ve Sn-Bi lehim pastasına kıyasla daha iyi temas açısıyla yayılma alanında önemli bir iyileşme görüldüğünü gösterdi. Yapılan çalışmada epoksi ilavesi ile yapılan lehimlerin düşme testlerinde normal lehimlere göre çok daha dayanıklı olduğu gözlemlendi. İdeal olduğu düşünülen ağırlıkça %5 epoksi katkısı bulunan lehimin epoksi katkısı bulunmayan lehime göre 2.6 kat daha dayanıklı olduğu gözlemlendi. Bu sebeple uzaya gönderilen araçlar veya yüksek titreşime maruz kalacak yapılarda epoksi ilaveli lehimlerin kullanılması lehim dayanımı açısından önemli bir avantaj sağlayacaktır. Ayrıca Sn-Bi lehim pastasının dış yüzeyinin epoksi polimer ile kaplanması aynı zamanda dış etkenlere karşı koruyucu bir kalkan görevi de görmektedir. Epoksinin farklı yüzeylere tutunabilme özelliği sayesinde lehim pastasının farklı yüzeylerde lehimlenmesini sağlar.

Anahtar Kelimeler: Sn-Bi lehim pastası, epoksi reçine, temas açısı, yayılma alanı

CONTENTS

NOMENCLATURE

Acronyms

DSC	Differential Scanning Calorimeter
SEM	Scanning Electron Microscope
EDX	Energy Dispersive X-ray Spectroscopy
IMC	Intermetallic Compound
Zn@Sn	Sn coated Zn
mN	Millinewton
Sn-Pb	Tin-Lead
SAC	Tin-Silver-Copper
SAC305	0.5% copper, 3% silver and 96.5% tin
Sn-58Bi	42 wt.% tin 58 wt.% bismuth
Ag	Silver
Ti	Titanium
Co	Cobalt
In	Indium
BPA	Bisphenol A
OH	Hydroxide
$BaTiO_3$	Barium titanate
$C_{15}H_{16}O_2$	2,2-Bis (4-hydroxyphenyl) propane
θ	Contact angle

µm	Micrometer
KHz	Kilohertz
mm	Millimeter
T_{max}	Temperature maximum
T_{min}	Temperature minimum
°C	Degree Centigrade
γ_{gs}	Gas/solid surface tension
γ_{ls}	Liquid/solid surface tension
γ_{gl}	Gas/liquid surface tension
W_{ad}	The adhesion work
S_R	Spreading ration
D	Diameter of sample
SE	Secondary electron
BSEs	Backscattered electrons

LIST OF TABLES

LIST OF FIGURES

CHAPTER 1

INTRODUCTION

Since lead, a heavy metal, is harmful to human health, its use is restricted or banned. Steps have been taken to restrict the use of lead in Europe, which came into force in 2006. Therefore, this ban caused major problems in reflow soldering at that time. We can say that the surface mount technology industry was the most affected at that time [1]. Before the ban, Sn-Pb (tin-lead) alloys were preferred due to their low surface tension [2], good mechanical properties [3] and low melting point [4]. At first, solder pastes contained SAC (tin-silver-copper) were preferred instead of solder paste containing lead [5]. SAC305 (0.5% copper, 3% silver and 96.5% tin), a type of alloy with a high melting temperature of 218 °C. Considering the reflow temperature of this alloy, it becomes re-solderable when subjected to temperatures of 240 °C – 270 °C [6]. This temperature requirement requires high carbon dioxide emissions and high energy consumption. This situation is not a desired situation when considered in industrial terms. Due to this situation, researchers have started to make solder paste with alloys with different components. A few typical lead-free solders are shown in Figure 1.1.

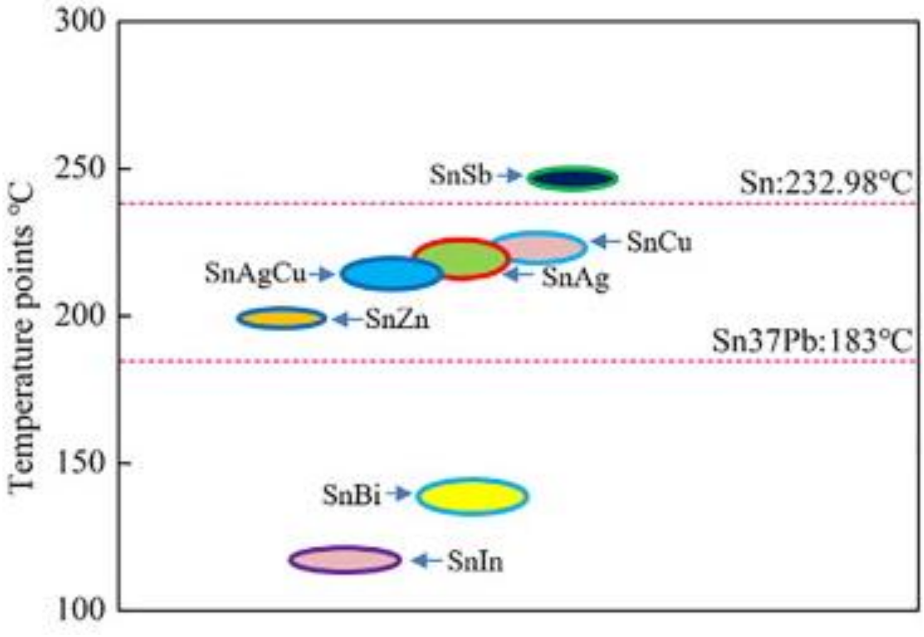

Figure 1.1 A few typical lead-free solders [7]

However, the Sn-Bi (tin-bismuth) alloy has eutectic melting point of 138 °C. Sn-Bi equilibrium phase diagram is shown in Figure 1.2. This will reduce energy consumption and carbon dioxide emissions. That's why we chose Sn-Bi solder paste due to both its cost and its ability to be soldered at low temperatures.

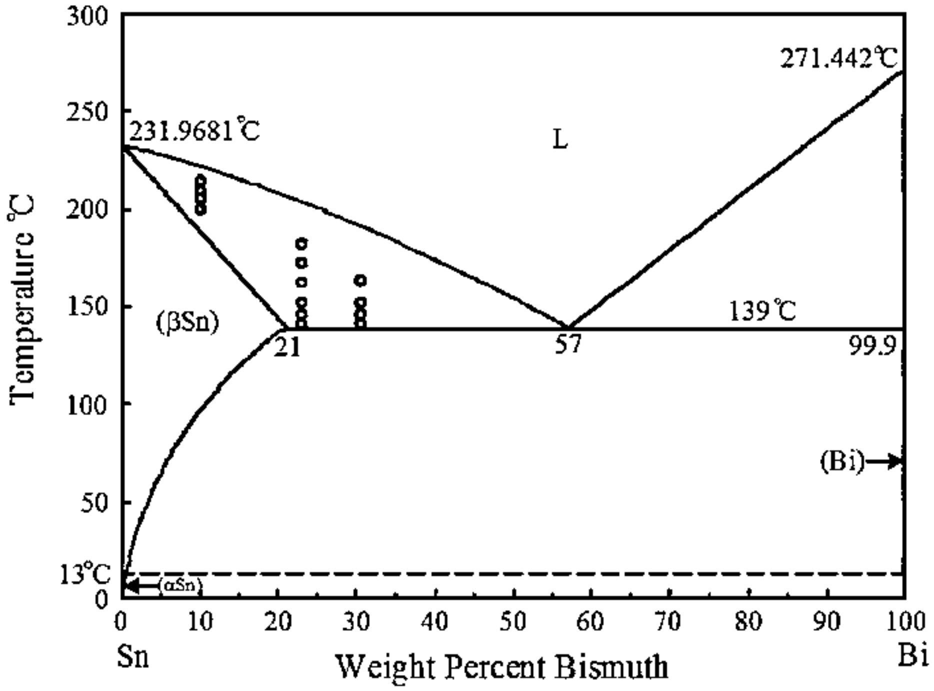

Figure 1.2 Sn-Bi equilibrium phase diagram [8]

1.1 Sn-Bi Solder Paste

After the use of lead in solder pastes was banned, manufacturers turned to solder pastes with different structures. Solder paste is a structure consisting of metal solder particles, a combination of powder and paste-like adhesive flux. The most important feature of solder paste is that it can be soldered easily. Sufficient solder paste is applied to the surface, then the applied surface is heated enough to re-flow and the soldering process is completed. In this way, it is possible to obtain a very durable solder by using solder paste compared to normal soldering methods. In this context, it is possible to see at what temperature the Sn-Bi solder paste we have chosen enters liquid form in different combinations with the help of differential scanning calorimetry (DSC). According to the DSC results, the liquid state temperatures of Sn-Bi solder paste in different compositions are included. Liquidus temperature, solidus temperature and solidification interval for different Sn-Bi solder alloys are shown in Table 1.1.

Table 1.1 Liquidus temperature, solidus temperature and solidification interval for different Sn-Bi solder alloys.

Solder Composition	Solidus (°C)	Liquidus (°C)	Solidification Interval (°C)	Reference
Sn-35Bi	138.0	186.0	48.0	[9]
Sn-40Bi	138.0	178.0	40.0	[9]
Sn-45Bi	138.0	168.0	30.0	[9]
Sn-50Bi	138.0	155.0	17.0	[9]
Sn-55Bi	138.0	144.0	6.0	[9]
Sn-58Bi	140.3	146.0	5.7	[10]
Sn-58Bi	139.6	147.4	7.8	[11]
Sn-58Bi	139.4	148.0	8.6	[12]
Sn-58Bi	139.5	147.6	8.1	[13]
Sn-58Bi	139.3	147.6	8.3	[14]
Sn-58Bi	139.0	143.1	4.1	[15]
Sn-58Bi	136.1	139.1	3.0	[16]
Sn-58Bi	136.1	139.1	3.0	[17]
Sn-58Bi	130.2	139.0	8.8	[18]
Sn-58Bi-0.1Ag	136.2	139.7	3.5	[17]
Sn-58Bi-0.5Ag	135.7	138.2	2.5	[17]
Sn-58Bi-1Ag	137.0	176.0	39.0	[9]
Sn-58Bi-1Ag	137.0	142.0	5.0	[9]
Sn-58Bi-2Ag	139.1	145.4	6.3	[11]
Sn-58Bi-0.5Ti	138.9	142.7	3.8	[15]
Sn-58Bi-1Ti	139.1	143.4	4.3	[15]
Sn-52Bi-1Sb	140.6	168.7	28.1	[12]
Sn-58Bi-1.4Sb	141.2	170.4	29.2	[12]
Sn-48Bi-1.8Sb	140.9	172.7	31.8	[12]
Sn-44Bi-1.8Sb	141.9	180.5	38.6	[12]
Sn-48Bi-1.8Sb	140.6	152.0	11.4	[12]
Sn-48Bi-2Sb	142.2	169.6	27.4	[12]
Sn-48Bi-2.4Sb	142.9	169.3	26.5	[12]
Sn-48Bi-2.8Sb	143.6	168.4	24.8	[12]
Sn-40Bi-0.1Cu	125.1	132.2	7.1	[18]
Sn-58Bi-0.5Co	140.1	145.0	4.9	[10]
Sn-58Bi-2In	129.7	135.0	5.3	[11]
Sn-58Bi-3In	119.8	140.4	20.6	[11]

Based on the table containing the DSC results, we can say that the transition temperature of Sn-58Bi alloys to the liquid phase is between 139 °C - 147.6 °C. The main disadvantage of Sn-58Bi alloys is that they have a brittle structure due to the natural properties of bismuth [19]. To eliminate this brittle structure, we produced epoxy polymer reinforced Sn-58Bi solder paste. Thanks to the epoxy polymer, we had a cured layer. This both protects us from external factors and eliminates the problems caused by the fragile structure of bismuth. This shows us that we have actually obtained a composite solder paste.

1.2 Epoxy Polymer

Epoxies are formed as a result of cross-linking of the curing agent and epoxy resin [20]. Therefore, epoxies are a thermosetting polymer. Thermosetting polymers are a type of polymer that is irreversibly. Once it is shaped and cured, it is not possible to put it into a different form again. Epoxy resins are named after the epoxy functional groups in their structure. Epoxy functional group are shown in Figure 1.3.

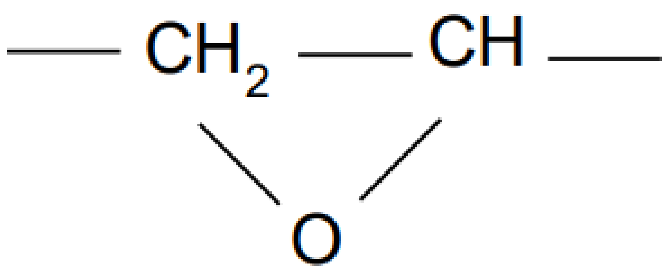

Figure 1.3 Epoxy functional group [21]

Cross-links are formed as a result of the hydroxyl groups and epoxy groups contained in epoxy resins reacting with the second component, which is called a hardener or curer, and these bonds ensure the structure is solid. These cross-links do not allow reflow of the polymer. Epoxy has very high resistance to chemicals, water, burning, and alkaline substances [21,22]. Its biggest advantage is that epoxy does not undergo a volumetric change after hardening and maintains its original state [23]. The size of the product does not deteriorate. Epoxy product has high resistance to fatigue. Thanks to its ability to adhere to epoxy surfaces, it can combine different products and preserve them securely [24]. It is a polymer structure whose hardness and flexibility are adjusted during the production phase of epoxy. Additionally, the toughness value of the product is very good [25].

Epoxy compounds can be obtained by two methods. The first is obtained as a result of the interaction of halogen hydrins with bases. Secondly, we can say that it is a process resulting from the oxidation of alkenes with peracids. Figure 1.4. and Figure 1.5. are also shown.

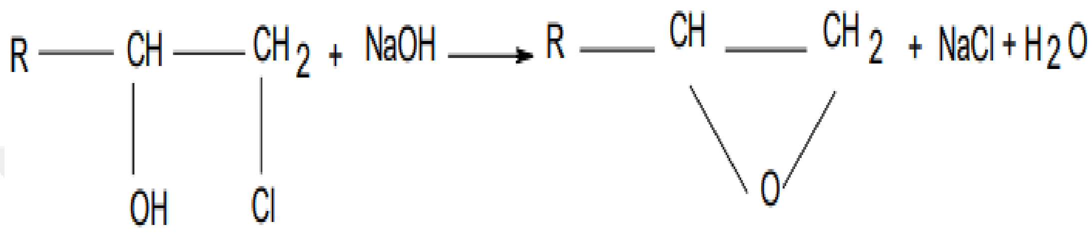

Figure 1.4 The epoxy compound formed by the reaction of halogens with bases [26]

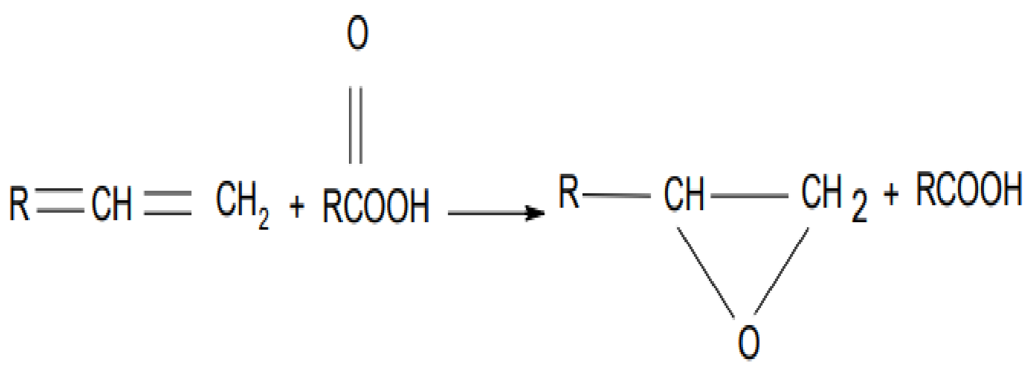

Figure 1.5 The epoxy compound formed by oxidation of alkenes with peracids [27]

1.2.1 Bisphenol A

The name of the Bisphenol A (BPA) polymer is 2,2-Bis (4-hydroxyphenyl) propane. Its molecular weight and formulation are $C_{15}H_{16}O_2$ = 228.29 g/mol. The production method is obtained by mixing acetone and phenol in sulfuric acid or hydraulic acid in a ratio of 2:1 and concentrating them by catalysis [28]. Bisphenol A is completely soluble in organic solvents. But it is very slightly soluble in water. Bisphenol A is a colorless and odorless type of polymer. Bisphenol A is the most widely used polymer group in the production of epoxy resins [29]. Chemical structure of bisphenol A are shown in Figure 1.6. Epoxy resin obtained from Bisphenol A has a viscous structure [28]. This ensures good adhesion and resistance to corrosion. Chemical structure of bisphenol A is shown in Figure 1.6.

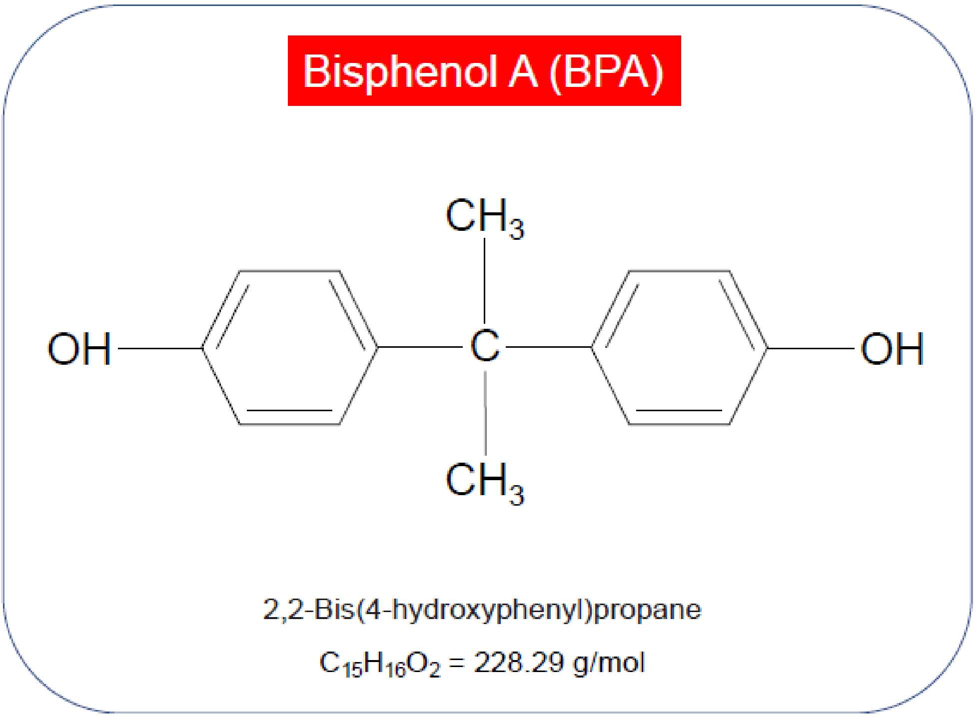

Figure 1.6 Chemical structure of Bisphenol A [30]

1.3 Curing Agents

Curing agents react with the OH group and as a result the polymers become cross-linked. Curing agents are generally auxiliary agents that help the product bond in whatever way it is desired to achieve the desired properties. Curing agents have a structure that makes the product flexible or harder. Curing agents are divided into the following subheadings.

1.3.1 Aliphatic Polyamines

We can give diethylene tetramine, ethylenediamine and triethylene tetramine as examples of aliphatic polyamines. Aliphatic polyamines can operate at low temperatures and low viscosity. When considered dangerous, aliphatic amines have a high molecular weight as a result of the reaction, which makes them more reliable. In general, if the epoxy system has low vapor pressure, amidoamine is used to strengthen the reactive polyamides, so that the structure becomes stronger [31,32]. Chemical structure of ethylenediamine and triethylene tetramine are shown in Figure 1.7 and Figure 1.8.

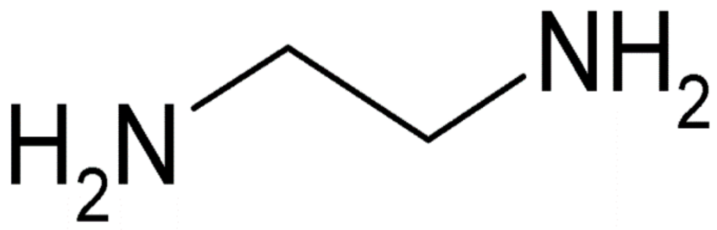

Figure 1.7 Chemical structure of ethylenediamine [31]

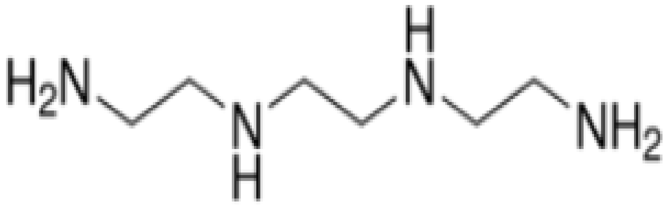

Figure 1.8 Chemical structure of triethylene tetramine [32]

1.3.2 Modified Aliphatic Polyamines

Room temperature is sufficient to synthesize curing agents of this class. Extrafollicular amines and the components of the resin react in the epoxy resin. In this case, amines decrease and the molecular weight increases inversely with the decrease in amines. Aliphatic polyamines and amine curing systems have the ability to be mixed [33].

1.3.3 Aromatic Amines

Most commonly used aromatic amines are m-phenylenediamine, 4,4-diaminodiphenyl sulfone and 4,4-methylenedianiline. Aliphatic amines are more reactive than the other amine group, aromatic amines, and requires 149 °C for the curing process [34]. Chemical structure of 4,4-methylenedianiline and 4,4-diaminodiphenyl sulfone are shown in Figure 1.9 and Figure 1.10.

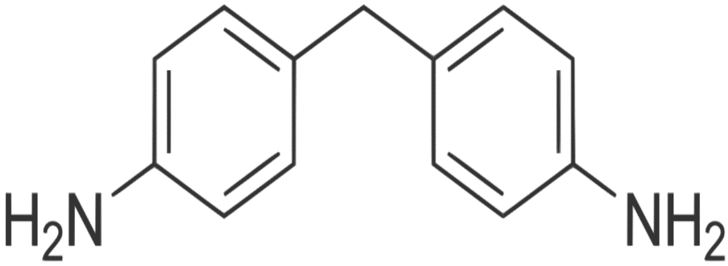

Figure 1.9 Chemical structure of 4,4-methylenedianiline [34]

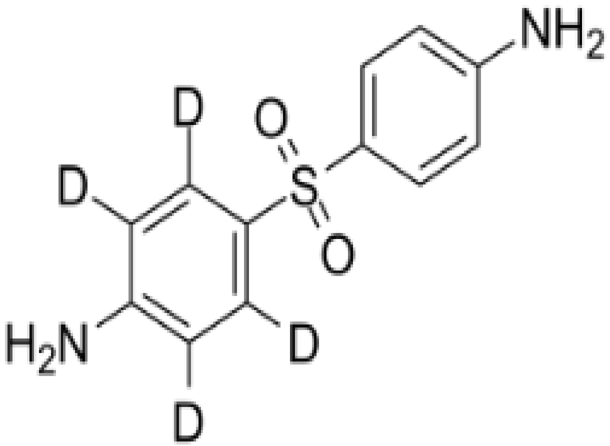

Figure 1.10 Chemical structure of 4,4-diaminodiphenyl sulfone [34]

1.3.4 Carboxylic Acids

It is a curing agent formed as a result of cross-linking of carboxylic acid-based epoxy resins. The component that stabilizes the functional groups is the OH group. It reacts epoxy resins to form stabilized [35]. Chemical structure of carboxylic acid is shown in Figure 1.11.

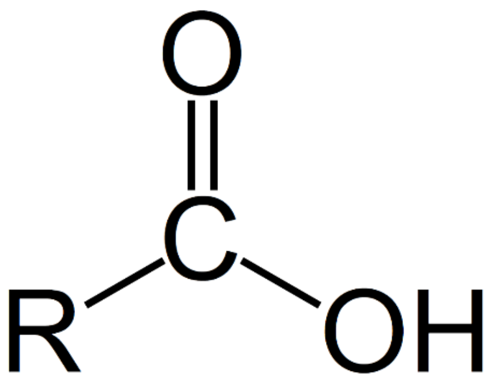

Figure 1.11 Chemical structure of carboxylic acid [35]

1.3.5 Acid Anhydrides

It is the second most preferred curing agent. Its electrical properties are better when compared with aromatic amines. However, it requires higher temperatures than aromatic amines. Commonly used acid anhydrides include methylenedic anhydride, trimellitic acid, and thallium [36,37]. Chemical structure of trimellitic acid is shown in Figure 1.12.

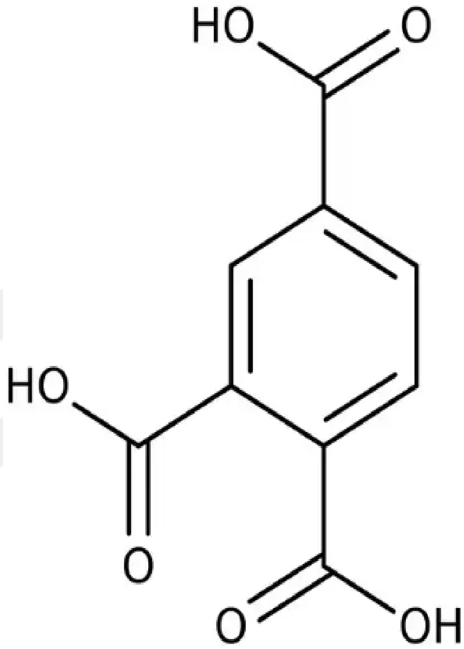

Figure 1.12 Chemical structure of trimellitic acid [36]

1.4 Review of Related Works

Fengjiang et al. [38] studied the mechanical properties and interface reaction of Sn-Bi solder joints. Information is given about the differences in Sn-Bi solder paste as a result of increasing the amount of bismuth added by weight and how this affects the structure of the solder. Within the scope of this information, it has been observed that the lower the content of bismuth, the soldering temperature increases inversely proportional to it until the eutectic bismuth value is reached. Bismuth provided the lowest soldering temperature when it had eutectic tin bismuth content. It shows that excessive adding of bismuth triggers morphological fracture and increases the shear strength of the solder joint.

Asit et al. [39] examined the effect of nanoparticle-added nickel on the mechanical properties of Sn-Bi solder paste. When the pure Sn-Bi solder paste was soldered to the Cu surface, an island-shaped Cu6Sn5 intermetallic compound (IMC) layer was detected. However, thanks to the added nickel nanoparticles, the formation of Cu6Sn5 was prevented. In this case, Sn-Ni provided IMC formation. Thanks to this formation, the formation of compounds between copper and tin was prevented. Sn-Bi provided the solder paste with better mechanical properties.

Hui-Wei et al. [40] studied conditions that occur in the microstructure as a result of the aging process of Sn-Bi solder paste and Sn-Bi-Cu solder paste. These two solder pastes were aged by subjecting them to 100 °C heat for 100 days. At the end of this process, the microstructures were examined and coarsening was observed in the Bi phase of the Sn-Bi solder paste. However, it turns out that adding copper to the Sn-Bi-Cu solder paste significantly reduces Bi coarsened.

Yang et al. [41] examined the improvements in mechanical properties of Sn-58Bi solder paste as a result of as-reflowed. During the re-soldering process, the grain size of the β-Sn phase increased as the product is exposed to high temperatures. In this case, it causes the elastic modulus and hardness of the solder to decrease.

Hyejun et al. [42] touched upon the effects of alloying and nanoparticle addition to Sn-Bi solder paste in terms of mechanics and microstructure. Addition of Co, Ti and Ag to Sn-Bi solder paste does not cause a change in melting temperature. However, adding Indium (In) lowers the melting temperature. Addition of Sb increases the melting temperature of Sb-Bi solder paste. Addition of alloying elements such as Cu, Ag, In and Sb in ideal proportions causes an increase in the wettability of Sn-Bi solder paste. However, high adding affects wettability negatively. When nanoparticles were added at the ideal ratio, positive results were obtained in elongation and tensile strength.

Fengyi et al. [43] examined the changes in the microstructure of Sn-Bi solder paste reinforced with Sn-coated Zn(Zn@Sn) particles as a result of thermal cycled. Zn added to Sn-Bi solder paste subjected to thermal cycling reduced the nucleation energy. It also contributed to improvements in the eutectic structure. It significantly reduced the coarsening of the bismuth-rich phase, which was expected to coarsen in this process.

Zn-rich phase structures were distributed in different places in the solder joints and did not move. In this case, it acted as a barrier and prevented the bismuth phase from diffusion from the hot end to the cold end.

Li et al. [44] examined the effects of adding nanosized graphite to Sn-Bi solder. The addition of nano-sized graphite to Sn-Bi solder pastes negatively affected the spreadability value. The added graphite caused a decrease in the tensile strength of the Sn-Bi solder. However, compared to Sn-Bi solder, the structure which contains nano-graphite showed better creep value. The reason for this is that nanosized graphite dislocations.

Xiao-Guang et al. [45] included the properties of Sn-58Bi solder with epoxy content. Epoxy additive resulted in a positive improvement in the wettability of Sn-Bi solder paste. Because solders with a curable flux system contained volatile substances, which negatively affected fluidity. However, epoxy-containing solders have good fluidity due to the absence of volatile substances. An improvement of 1/4 was achieved in the shear strength of epoxy-containing Sn-Bi solder.

Li et al. [46] examined the effects of adding nanoparticle-sized $BaTiO_3$ to Sn-Bi solder on the microstructure and mechanical properties of the solder. Different weight percentages of $BaTiO_3$ were added and their effects on Sn-Bi solder paste were examined. In this study, the best soldering angle was $BaTiO_3$ with a content of 1% by weight. Additionally, $BaTiO_3$ additives up to 3% improved the mechanical properties of Sn-Bi solder. Finally, it can be said that $BaTiO_3$ added 1% by weight improves the ductility of the solder to a certain extent.

Cheng et al. [47] examined the effects of adding Sb to Sn-Bi solder on the properties of the solder. First, when the added Sb content is increased, the soldering temperature increases. However, when a certain threshold is exceeded, the soldering temperature decreases. The main reason for this is due to the decreasing Bi content. The addition of Sb significantly affects the spreading area of the solder, but Bi does not have any effect on the spreading area. The best spreading rate was obtained by adding 2% Sb by weight. It is thought that when this ratio increases, the shear strength will increase.

Here we can say that the Sb ratio, when used correctly, has a significant positive effect on the structure of the solder.

Meng-Ying et al. [48] examined the solder ball spatter formation and dynamic wetting behavior of Sn-Bi solder paste in the reflow soldering process. When Cu is subsequently added to the Sn-Bi solder paste, solder ball spatter is observed when exposed to reflow. The way this occurs is if there is un-melted solder powder in the solder pastes, this powder pushes the melted solder towards the corners, which causes solder ball smearing. Other precursor metals that cause solder ball spatter originate from Bi solder balls obtained as a result of the redox reaction of Bi, and Sn oxides.

Fu et al. [49] examined the resistance change occurring in the solder during the electromigration process of Sn-58Bi solder. As a result of this article, a valley structure is observed on the surface where the cathode was located. This structure shows that the resistance increases gradually over a long period of time. However, in the later process, it suddenly jumps in places where the free surface solder was connected. In terms of microstructure, it was observed that Bi and Sn-rich phases were present in high-temperature solders. Additionally, no change was observed in the microstructure of the solder at low temperature. This did not cause a change in resistance.

Xin et al. [50] examined how the Sn-Bi alloy solder affects the electrical resistance depending on temperature. Resistivity increases with increasing temperature and increasing bismuth. At temperatures below 70 °C, the resistivity increases linearly depending on the temperature. However, at temperatures above 80 °C, bismuth dissolved faster than tin, caused greater sensitivity to temperature. This causes solder not to give reliable results if used at high temperatures. For example, the results of an experiment held below 70 °C differ from the results of an experiment conducted above 80 °C. The biggest reason for this is changes in the microstructure.

1.5 Aim of the Study

Today, leaded solder is prohibited by European standards. For this reason, interest in lead-free solders is increasing day by day. Commonly used solder pastes require higher temperatures of 50 °C and above for the soldering process compared to the Sn-58Bi solder pastes used in the project. This difference is quite high considering the temperatures at which the soldering process takes place. We can say that the solder paste composition to be used in this study is a composition that can be soldered at low temperatures. In this way, it will be possible to reduce the amount of energy used and thus prevents a large energy loss. It has a suitable contact angle for surface soldering and offers the possibility of layered soldering by choosing solder with more than one melting temperature on the same electronic board. Otherwise, desoldering all components at the same time may cause problems in production.

One of the biggest problems with Sn-Bi solder pastes without epoxy polymer additives is that bismuth easily oxidizes during the reflow soldering process. This creates black oxide and affects solder joint performance. It is possible to say that black residue has been reduced or even completely eliminated thanks to the flux used in the project. The second problem is that external factors cause the solder to interact with the surface and the solder composition to change over time. To prevent this, we created a polymer layer on the surface by adding a certain amount of epoxy resin to our solder paste. Thanks to this situation, the solder has become very resistant to external factors. In addition, thanks to this layer, it is possible to prevent cracks in the solder. In this way, it is aimed to significantly increase the service life of the solder. In addition, thanks to the added epoxy, the solder angle decreased. This decrease shows us that the soldering ability has increased even more. In this way, the solder will show better structural properties.

Another important issue is to ensure that the solder can be soldered to different surfaces. Because solders generally enable soldering between two metals. However, solder paste containing epoxy is famous for its ability to be applied to different surfaces thanks to the high adhesion properties of epoxy. In addition, protection of the soldering surface against external factors thanks to the polymer layer on the outer surface is a very important development.

CHAPTER 2

EXPERIMENTAL PROCEDURE

2.1 Preparation of Sn-Bi Solder Paste

An alloy containing 42 wt% tin and 58 wt% bismuth was purchased. The procuring organization was BBIEN technology limited. The grain size of this purchased alloy was 20-38 μm. This powder form was used in solder paste. The flux was added after purchasing the desired size powder. The flux was supplied by the same company. The flux selected was the solder flux compatible with Sn-Bi powder. Experiments were made with the selected flux and the amount of flux to be added was determined. Solder paste are metal powders with 88.5% metal by weight and 11.5% flux by weight. The points taken into consideration when finding this ratio were the contact angle of the solder and solderability. When less was added, a very high soldering angle was obtained. It was observed that the solder did not melt at the desired temperature when it was lightly added. Additionally, the soldering angle was high. Thanks to the added flux, the soldering angle decreased to the desired value range. Sn-Bi phase diagram. are shown in Figure 2.1. By looking at the phase diagram, we can say that the melting temperature will be 139 °C.

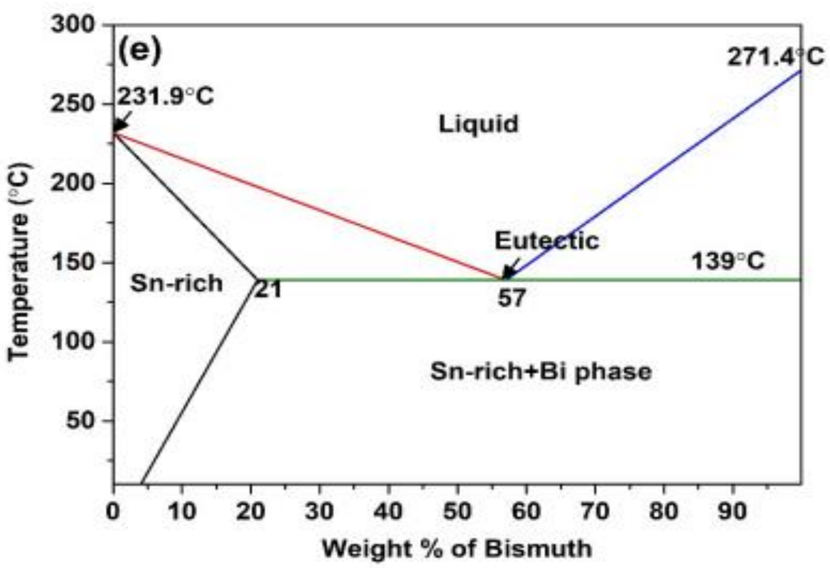

Figure 2.1 Sn-Bi phase diagram [51]

2.2 Obtaining Epoxy Polymer

The first of all, epoxy polymer used was an epoxy polymer belonging to the bisphenol a group. It was an epoxy polymer obtained from bisphenol-A and epichlorohydrin. We added curing agent to this epoxy polymer. The curing agent used was an aromatic amine compatible with the epoxy used. This aromatic amine was chosen by the supplying company. Our supplier company was marker resin technologies company. Epoxy resin and curing agent were mixed in the recommended ratio. This ratio is 3:1. As a result of this mixture, air bubbles were observed in the epoxy. We placed the epoxy polymer in an ultrasonic bath to remove these air bubbles. The temperature value used in the ultrasonic bath used was 32 °C. Under this temperature, the epoxy polymer stood for 10 minutes. The applied frequency is 53 KHz. Machine power was set to 60%. The used ultrasonic bath is shown in Figure 2.2.

Figure 2.2 The used ultrasonic bath

2.3 Adding Epoxy to Solder Paste

Epoxy polymer was added to the resulting solder paste. 1 wt.%, 3 wt.%, 5 wt.%, 7 wt.%, and 9 wt.% flexible epoxy polymer was added to the resulting solder paste, respectively. In order to added epoxy polymer to be soldered to an equal amount of copper surface, holes with a thickness of 1 mm and a diameter of 4 mm were created from the aluminum plate. As a result of placing equal amounts of solder paste through these holes, equal amounts of solder paste were placed in all trials. Figure 2.3 shows an aluminum plate that allows equal amounts of solder paste to be placed on the copper plate.

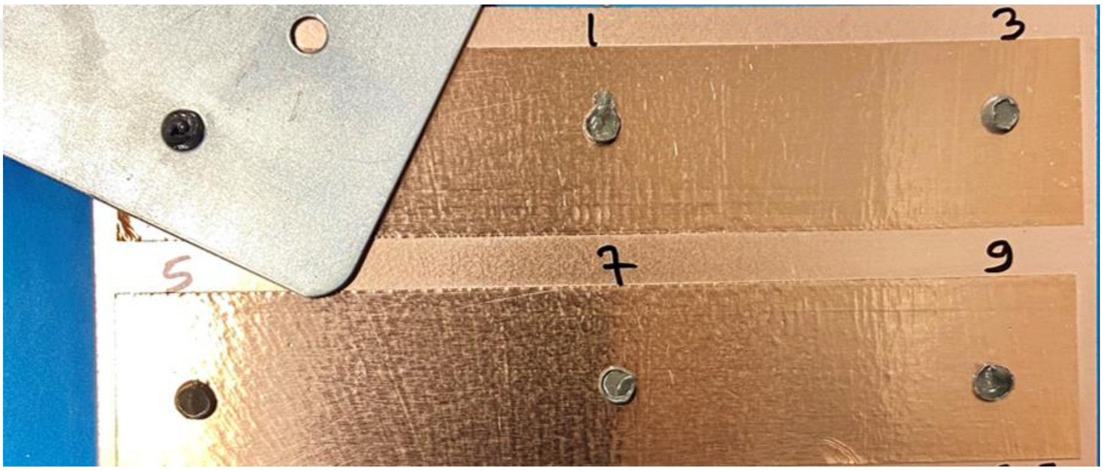

Figure 2.3 Aluminum plate that allows equal amounts of solder paste to be placed on the copper plate

2.4 Soldering Process to Copper Surface

In order to the soldering process to be good, the correct temperature and ambient conditions are required. When the correct temperature is given to the solder paste, first of all, the flux in the solder paste flows outward. The solder starts to flow 20 seconds after the flux flows out. The solder will completely flow after 30 seconds and solder the surface. The average soldering time with the generally used Sn-Bi solder paste is 90 - 100 seconds. The temperature value at which we applied was 160 °C for soldering. This is because we want to apply the same heat to each sample due to the epoxy. During this process, the volatile substances in the flux will first leave the environment. After soldering, the surface of the solder paste with flux content must be cleaned. Because when the flux is not cleaned, it will cause blackening after a certain period of time. Therefore, after soldering, the surface is cleaned with isopropyl alcohol

($CH_3CH(OH)CH_3$). Thus, only solder remains on the surface. Heat-blown soldering iron used in this study for the soldering process shown in Figure 5.

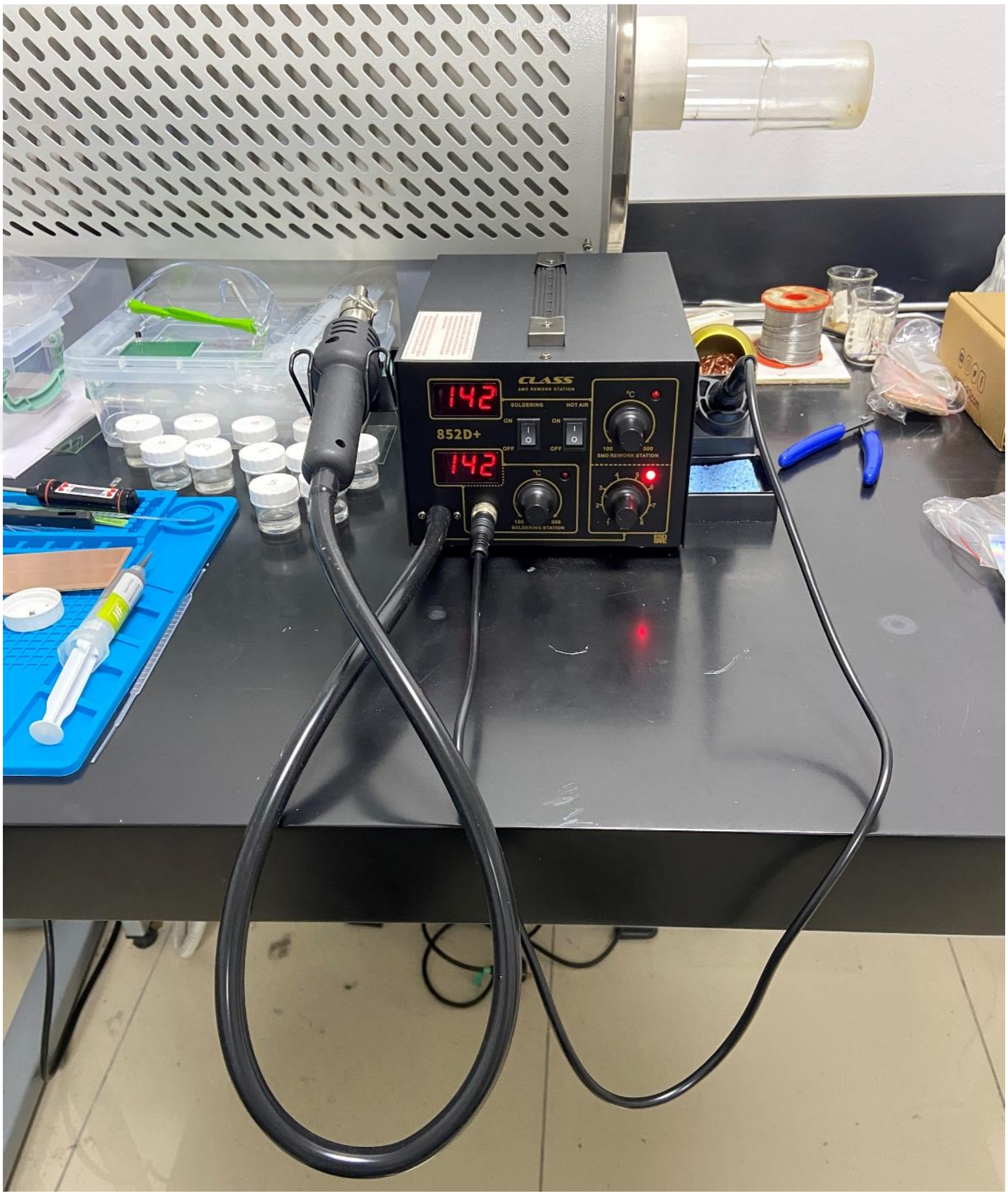

Figure 2.4 Heat-blown soldering iron used

Table 2.1 Applied treatments on samples

Sample Number	Solder paste content	Epoxy content by weight	Treatment
1	Sn-58Bi	0%	Sun exposure
2	Sn-58Bi	1%	Sun exposure
3	Sn-58Bi	3%	Sun exposure
4	Sn-58Bi	5%	Sun exposure
5	Sn-58Bi	7%	Sun exposure
6	Sn-58Bi	9%	Sun exposure
7	Sn-58Bi	0%	Sun exposure
8	Sn-58Bi	0%	100 °C oven for 3 days
9	Sn-58Bi	1%	100 °C oven for 3 days
10	Sn-58Bi	3%	100 °C oven for 3 days
11	Sn-58Bi	5%	100 °C oven for 3 days
12	Sn-58Bi	7%	100 °C oven for 3 days
13	Sn-58Bi	9%	100 °C oven for 3 days
14	Sn-58Bi	0%	Only soldered
15	Sn-58Bi	1%	Only soldered
16	Sn-58Bi	3%	Only soldered
17	Sn-58Bi	5%	Only soldered
18	Sn-58Bi	7%	Only soldered
19	Sn-58Bi	9%	Only soldered
20	Sn-58Bi	0%	One step soldering
21	Sn-58Bi	0%	Double step soldering
22	Sn-58Bi	0%	Thermal Cycling
23	Sn-58Bi	1%	Thermal Cycling
24	Sn-58Bi	3%	Thermal Cycling
25	Sn-58Bi	5%	Thermal Cycling
26	Sn-58Bi	7%	Thermal Cycling
27	Sn-58Bi	9%	Thermal Cycling

Table 2.1 shows the applied treatments to the samples. From sample number 1 to 7 samples were exposed to the sun. Samples 8 to 13 were exposed to 100 °C oven for 3 days. Samples 14 to 19 were not exposed to additional treatment they were only soldered. Samples 14 to 19 were used for soldering angle and spreading area. Sample number 20 soldered one time. Sample number 21 soldered two times. Samples 22 to 27 were treated with thermal cycling.

2.5 Thermal Cycling Test

Thermal cycling testing of solder joint is a test used to determine the ability of solder interconnects and analyze mechanical stresses caused by extremely varying high and low temperatures. A thermal cycle with a test condition between T_{min} (temperature minimum) -20 °C and T_{max} (temperature maximum) 100 °C was used. The duration of each cycle was 22 minutes, and the duration of stay at high and low temperatures was 10 minutes. The sample is kept at room temperature for 2 minutes while changing from hot to cold air. This thermal cycling test was repeated 400 times. As a result of this test, it tested what differences the solder joints will showed. Additionally, it is planned to perform a thermal shock test. In this method, the durability of the solder joint tested by cooling the surface of the solder joint with dry ice (-78.5 °C) and then exposing it to a temperature of 100 °C at a time. The solders were also placed in a 100 °C oven for 3 days. As a result, the changes in the samples were analyzed. After these tests, the surface was examined with the help of an SEM microscope.

2.6 Sn-Bi Solder Paste Sun Exposure Test

It is a test based on exposing epoxy and non-epoxy solders to sunlight. This test is performed to examine the microstructure changes and conditions that may occur on the surface as a result of exposure to sunlight for 8 hours a day for 28 days. In addition, thanks to this test, it was tested whether the epoxy polymer will turn yellow or not. The air temperature during this test was in the range of 32-39 °C. The average temperature is calculated as 36 °C.

2.7 Contact Angle of Solder

Equations (2.1) through (2.3) of the Young-Dupre equations used to characterize the wettability [52,53]. The connection between adhesion work, metal surface energy, and contact angle. The schematic representation of molten solder wettability on a metal substrate is seen in Figure 2.5. An experimental measurement of the contact angle can be used to assess the wettability of lead-free solders [54,55]. In order to assess the wettability of solders, the contact angle values are crucial [56,57]. A value of $0^{\circ}<\theta<30^{\circ}$ indicates very good wetting, $30^{\circ}<\theta<40^{\circ}$ expresses good wetting, $40^{\circ}<\theta<55^{\circ}$

indicates acceptable wetting, $55^\circ < \theta < 70^\circ$ expresses poor wetting, and $\theta > 70^\circ$ indicates very poor wetting. The metric may be applied to assess lead-free solder's wettability.

$$\gamma_{gs} = \gamma_{gl} \cos\theta + \gamma_{ls} \quad \textbf{(2.1)}$$

$$W_{ad} = \gamma_{gs} + \gamma_{gl} - \gamma_{ls} \quad \textbf{(2.2)}$$

$$W_{ad} = \gamma_{gl} (1 + \cos\theta) \quad \textbf{(2.3)}$$

γ_{gs} : gas/solid surface tension

γ_{ls} : liquid/solid surface tension

γ_{gl} : gas/liquid surface tension

W_{ad} : theadhesion work

θ : contact angle

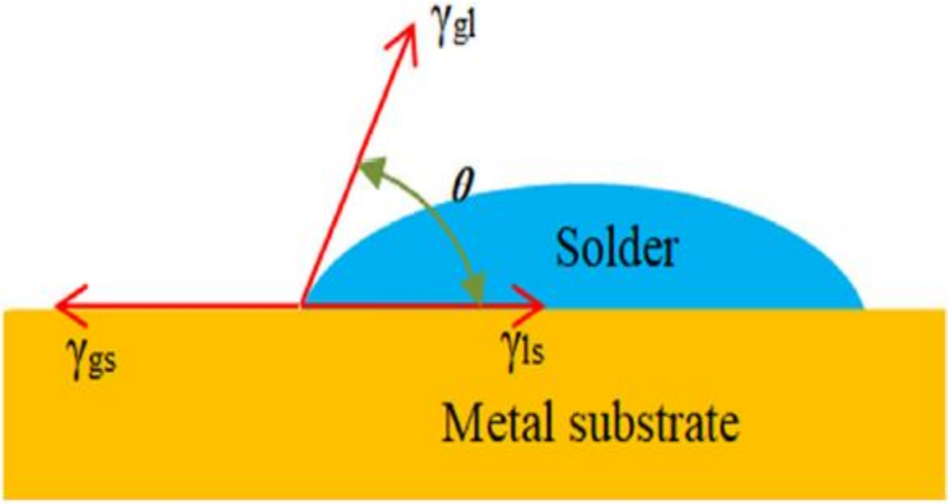

Figure 2.5 The wettability of molten solder on a metal substrate is shown schematically [54]

2.8 Spreading Area and Spreading Ratio of Solder

Lead-free solders' wettability may be assessed by using the spreading ratio [58]. The spreading ratio calculation equation is displayed as Equation 2.4 in accordance with the Japanese Industrial Standard JIS-Z3198-3 [59]. The lead-free solder's wettability improves with increasing spreading ratio [60]. In addition, the Chinese National Standard GB/T1136-2008 states that the spreading area of solder may be used to calculate the wettability of solder [61]. The distribution area of lead-free solder may be computed by software once the sample has been photographed and entered into a computer. The wettability calculation parameters are displayed in Figure 2.6. Solder's wettability correlated with its spreading area; this relationship used to examine how TiO2 nanoparticles affect the wettability. The impact of TiO2 nanoparticles on the wettability of Sn-Ag-Cu solder has examined, with the wider the spreading area, the better the solder's wettability [62]. It discovered that the 0.1 weight percent nanoparticles can increase solder's wettability.

$$S_R = \frac{D-h}{D} \text{ X } 100 \qquad \textbf{(2.4)}$$

S_R: spreading ration

D: diameter of sample

h: maximum height

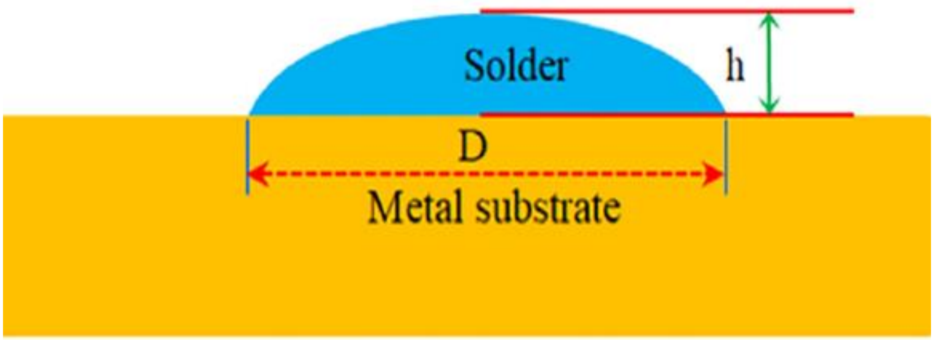

Figure 2.6 Wettability parameters for computation [60]

2.9 Drop Test for Sn-Bi Solder

The card level drop test designed as follows. First, the sample was prepared for the drop test. The prepared solder was fixed to the upper layer of the machine. The fixed solder sample was exposed to free fall movement. A device was developed to achieve the same speed and the same impact rate in all experiments. This device stops by hitting the samples from a height of 120 cm onto the rubber polymer on the ground with a fixed axis. It exhibits vibration movement during the stopping process. This test device is shown in Figure 2.7.

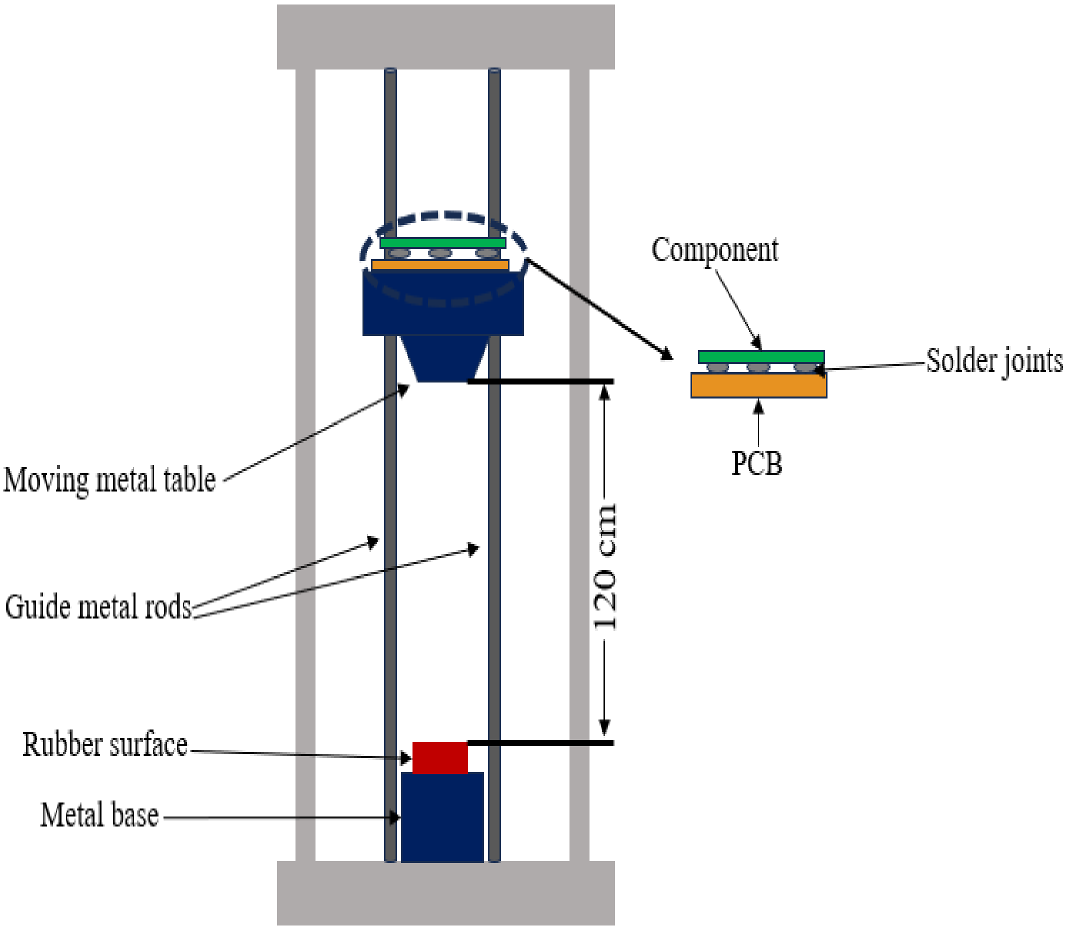

Figure 2.7 Schematic arrangement of the drop test device

In fact, it is the vibration movement that occurs after the fall that damages the solder. This vibration movement is the most important factor that damages the structure of the solder. Therefore, this test gives us an idea of how long it takes for the solder to lose its function depending on the conditions of use.

2.10 Characterization

2.10.1 Differential Scanning Calorimeter (DSC)

Differential scanning calorimetry measures variations in heat flow according to this principle. A sample whose temperature is gradually raised and then lowered was examined using DSC, and it was then contrasted with a reference probe. As a result, the enthalpies and melting points of any polymeric fiber can be found. In this case, changing the relevant parameters provides an opportunity to infer fundamental characteristics like equilibrium values; nevertheless, in terms of how the experiment is carried out, every parameter that could be changed must be carefully considered in order to do DSC appropriately. A furnace that has uniform heating and cooling capabilities is necessary for DSC. Two mountings for samples were located within this oven, and each mounting has a highly sensitive temperature sensor. Figure 2.8 illustrates the whole configuration.

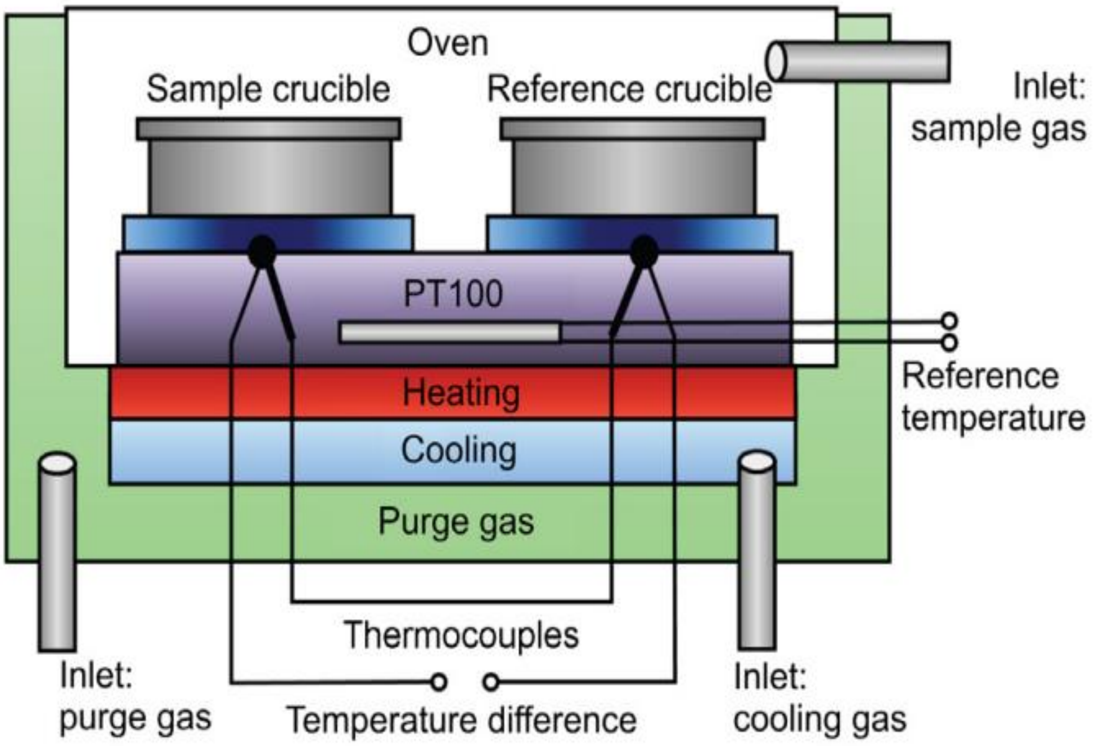

Figure 2.8 Schematic image of DSC [63]

The crucible holding the prepared sample has one mounting (left mounting in Figure 2.8). There is at least one opening in the crucible lid that allows for air exchange with the surroundings. Moreover, vaporization of sample particles prevents pressure build-up in the crucibles. An empty crucible was used as a reference in the other installation (right mounting in Figure 2.8). The final thermogram only shows effects that are induced by the sample itself because of the use of such a reference. To study transitions and chemical reactions in various atmospheres, a gas (sample gas) was used to purge the oven. During the DSC process, a protective gas (such as Ar or N_2) can be employed to establish an atmosphere surrounding the sample in order to prevent oxidation reactions. Otherwise, you can choose oxygen or air. In addition, a protective gas (N_2) was pumped into the area surrounding the oven to prevent ice formation in the winter [63].

2.10.2 Scanning Electron Microscope (SEM)

Scanning electron microscopy (SEM), produces high-resolution images of the subject. Using a scanning electron microscope, this procedure yields details on the object's composition and physical attributes. Anode, condenser lens, objective lens, scanning coils, and electron source are all crucial parts of the SEM apparatus. SEM images were captured with Hitachi's FlexSEM 1000 II device. The SEM device used can be seen in Figure 2.9.

The condenser lens and the scanning coils work together to regulate the beam produced by the electron source. Apertures may be used to modify the beam size, which determines the picture resolution. The objective lens focuses the beam into a single spot on the sample, while the scanning coils deflect the beam along the x and y axes.

SEM lenses are electromagnetic, made out of wire coils wound around metal poles. The magnetic field created by these coils manipulates electrons, giving the microscope control over them. When electrons contact with a sample, they can create two different forms of extra electrons: photons and irradiations. Imaging requires both secondary electrons (SEs) and backscattered electrons (BSEs). While BSEs are detected deeper and are more sensitive to changes in atomic number, SEs are reflected back when the main electron beam comes into contact with the sample element [64].

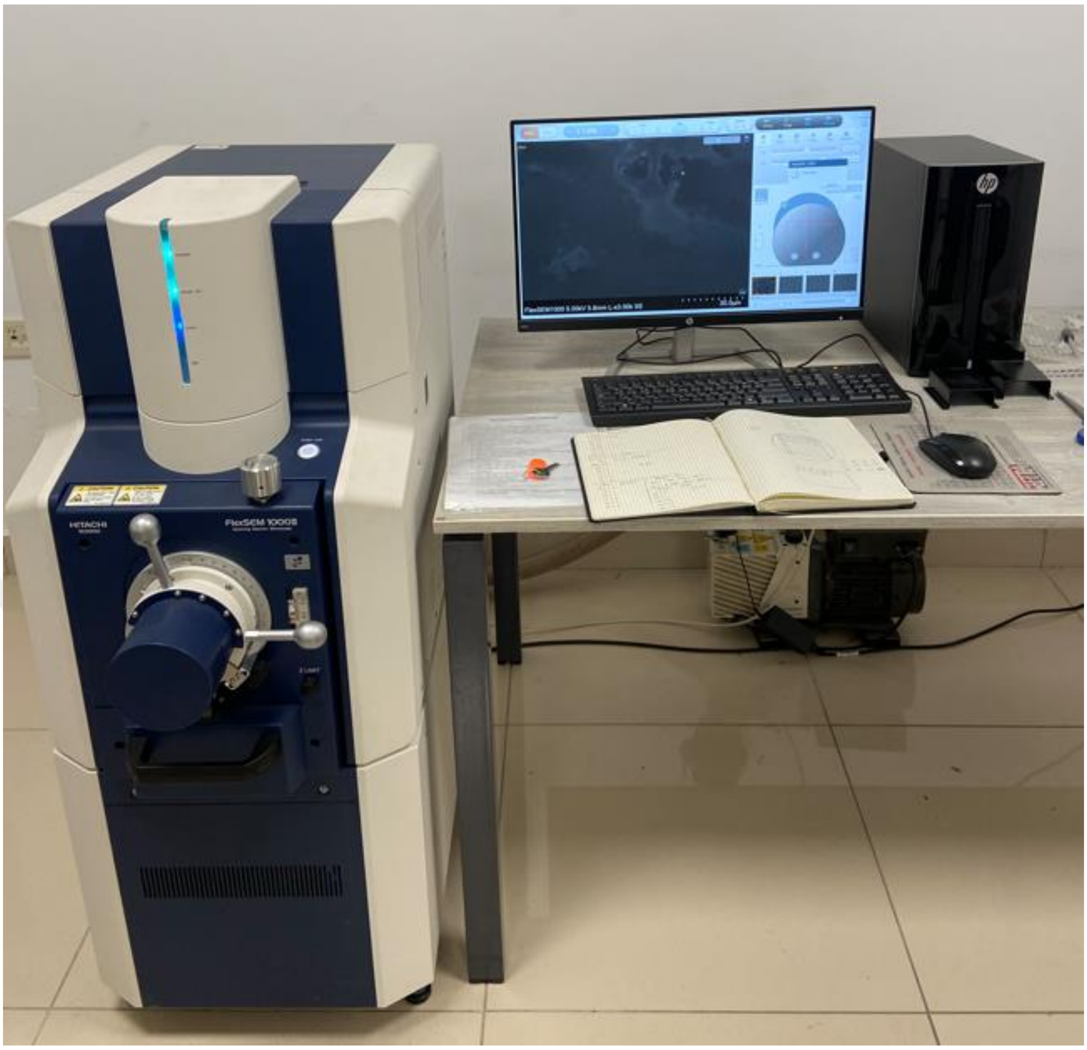

Figure 2.9 The used SEM device

The elemental composition of the structures may be ascertained both subjectively and quantitatively using energy dispersive X-rays, or EDX. This device was used to take images for Sn-Bi solder paste and Sn-Bi epoxy solder paste. Schematic diagram of a SEM is shown in Figure 2.10.

Sn-58Bi solders were prepared metallographically for SEM. The specimens were sanded with (1000, 1200, 1800, 2000, and 4000) silicon carbide emery paper. After this process, the samples were subjected to polishing. Polished with diamond suspensions. The samples were then etched with 3% diluted HCl. The samples were examined in SEM.

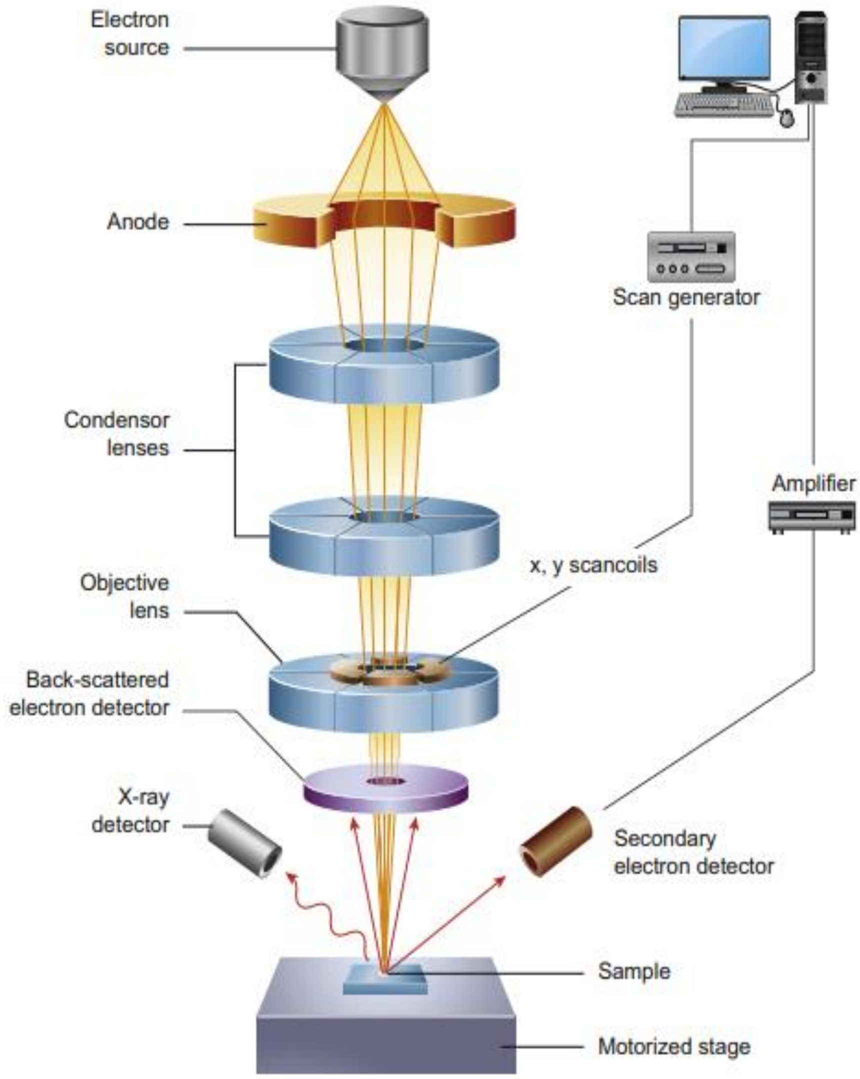

Figure 2.10 Schematic diagram of a SEM [64]

2.10.3 Hardness Measurement

Hardness is one of the most important properties to know about a material. Because there is a relationship between hardness and material mechanical properties. In Vickers hardness measurement, a tip harder than the material is immersed on the material with a certain time and load. In this method, a diamond pyramid tip with a square cross section and a peak angle of 136 degrees is used. As a result of this process, the indentation formed on the material is measured to find out which hardness degree these dimensions correspond to. The size measurement is done with an optical measurement. Soft and hard material hardness can be measured with Vickers hardness measurement

[65]. Figure 2.11 illustrates visuals related to this method. Within the scope of this study, HV 0.025 (245.2 mN) load was applied to the samples. Hardness values were measured with a Shimadzu digital micro-Vickers hardness tester. The hardness measuring device used in the tests is shown in Figure 2.12.

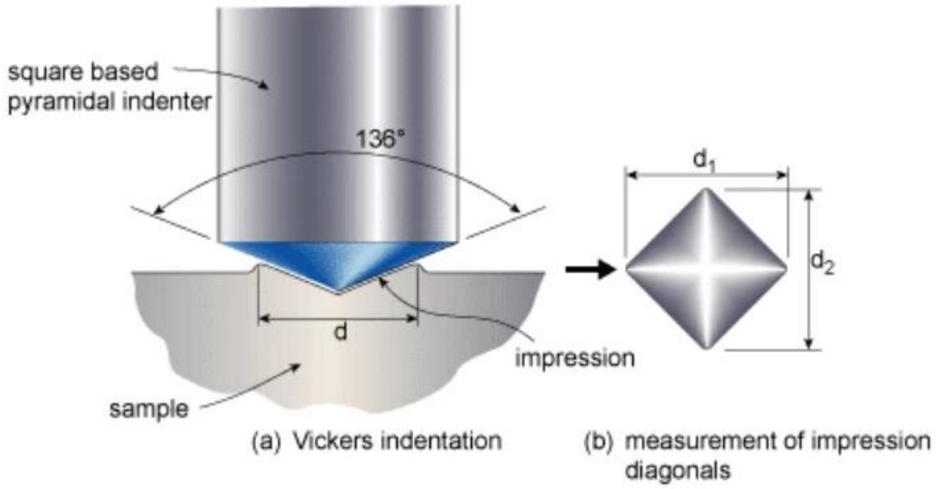

Figure 2.11 Vickers hardness measurement [65]

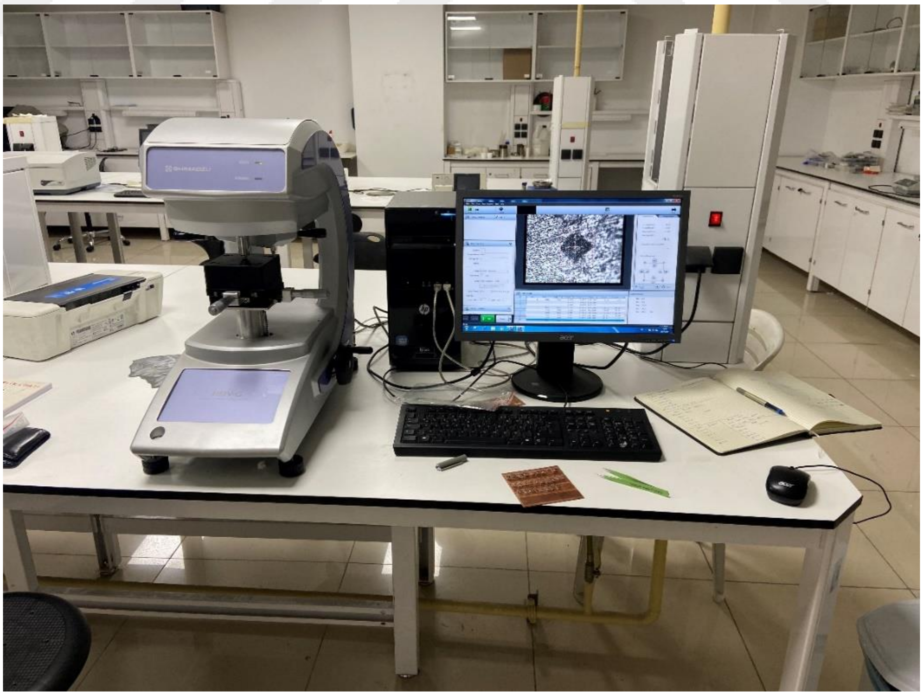

Figure 2.12 The hardness measuring device used in the tests

CHAPTER 3

RESULT AND DISCUSSION

3.1 Obtained Epoxy Polymer Result

In the epoxy preparation process, when epoxy resin and curing agent are mixed, a white wave structure is first obtained. At the end of the 5-minute mixture, we obtain a transparent epoxy. There are air bubbles in the epoxy mixture obtained. We can see these air bubbles in Figure 3.1.

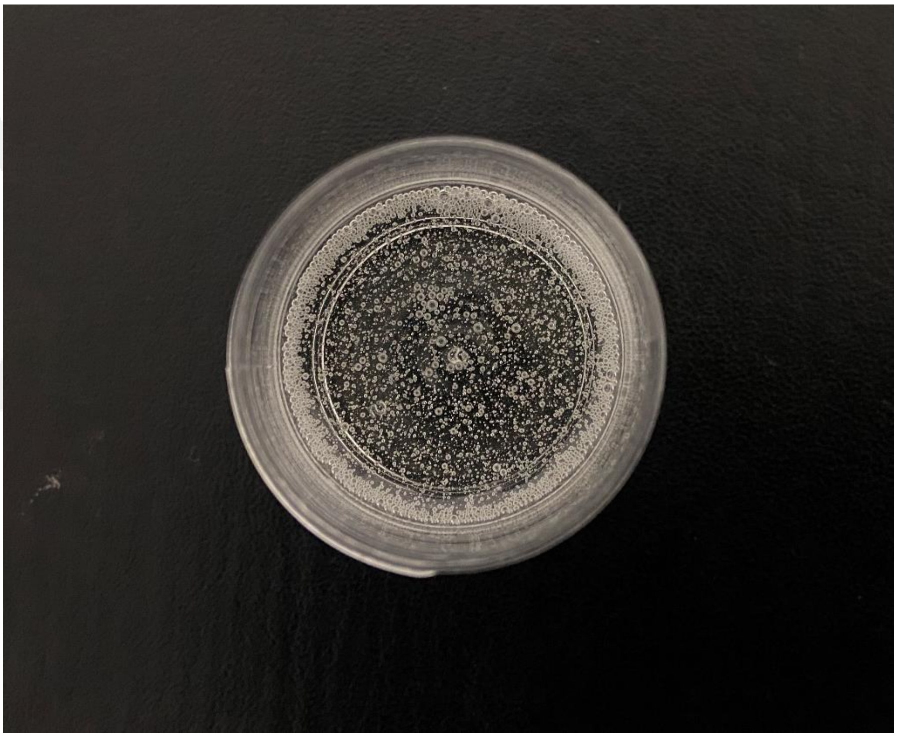

Figure 3.1 Epoxy containing air bubbles

To remove these air bubbles, we placed the epoxy polymer in an ultrasonic bath. The temperature used in the ultrasonic bath was 32 °C. Under this temperature, the epoxy polymer was kept for 10 minutes. The applied frequency is 53 KHz. The machine power was set to 60%. After this process, no air bubbles remained in the epoxy. We can see this in Figure 3.2.

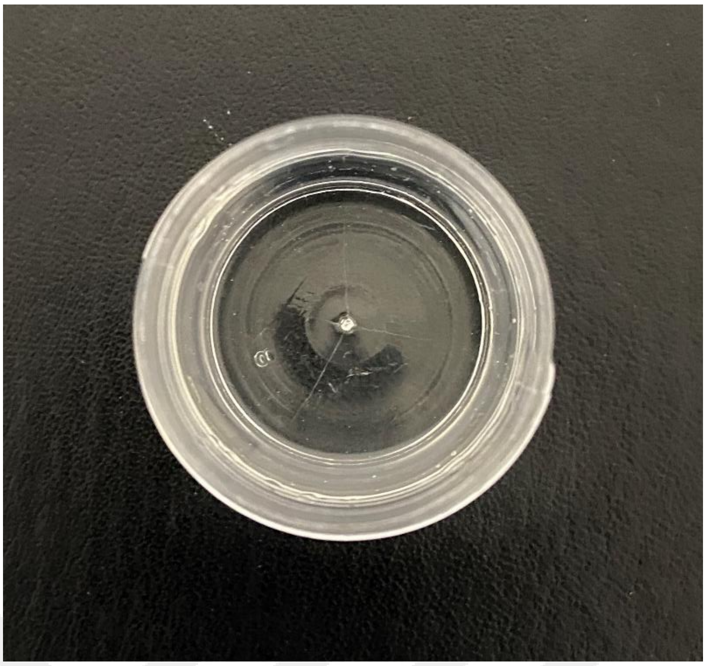

Figure 3.2 Air bubble free epoxy

3.2 Result of Soldering to Copper Surface

The soldering process was done in two different structures. The first is a solder paste without added epoxy. Secondly, epoxy added solder paste. These two solders are different from each other. Because the solder without epoxy addition will spread flux around during the soldering process. This spreading flux needs to be cleaned. Because it will darken after a certain period of time. Therefore, isopropyl alcohol was used as a surface cleaner. Thanks to the soldering station, we were able to solder our solder pastes easily. The soldering process was flux cleaned in epoxy-free solder pastes, which you can see schematically in Figure 3.3. A schematic representation of epoxy-containing solder paste can be seen in Figure 3.4. These two figures show the structure of the solder after soldering.

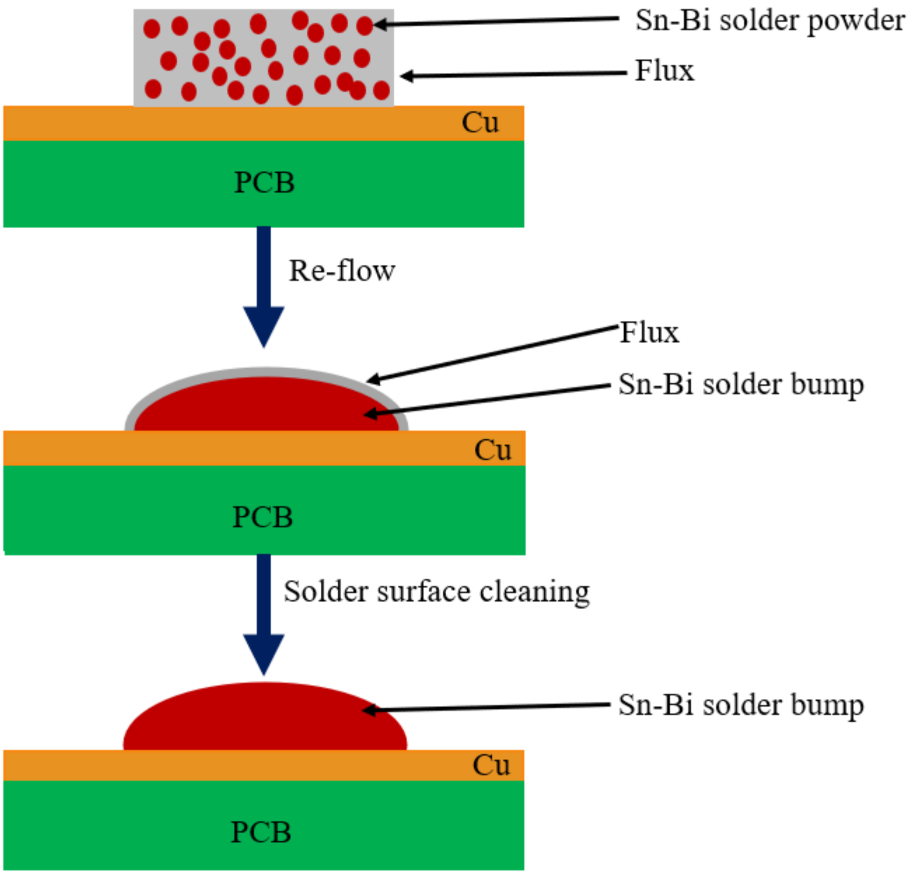

Figure 3.3 Schematic of flux-only Sn-Bi solder after soldering

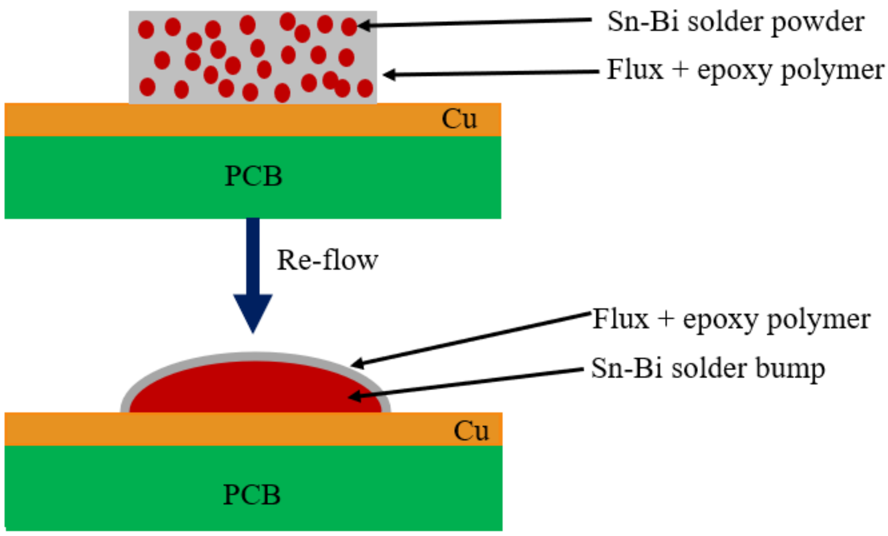

Figure 3.4 Schematic of Sn-Bi epoxy solder after soldering

3.3 Thermal Cycling Test Result

There was no visible change on the surface as a result of the thermal cycling test. This is due to the structure of the Sn-Bi solder obtained. Because bismuth has a relatively expanding structure as it cools. But Sn has a shrinking structure when it cools down. Therefore, it is possible to say that these two metals balance each other. There was also no deformation in the epoxy polymer. Because polymers have a thermosetting structure after curing, they do not undergo a change in shape. Visual inspection also did not reveal any negative results. This experiment was repeated 5 times and the products showed the same properties in all trials. We can see the sample in Figure 3.5.

Figure 3.5 Sn-Bi solders with different epoxy content

3.4 Sn-Bi Solder Paste Sun Exposure Test Result

After 8 days of exposure to the sun, the solder around the solder with no epoxy added darkened. This is due to the exposure of the flux to sunlight. No blackening occurred on the flux cleaned surface. The flux in this sample was not cleaned to see what would happen if the flux was not cleaned. No change was observed in the cleaned state. No interference was observed. This is because the temperatures exposed are low for solder. In fact, epoxy solder, which acts as a protective wall against all factors that will be exposed in the external environment, also dries against the sun. We can see the solder from Figure 3.6.

Figure 3.6 Sn-Bi solders with different epoxy content

3.5 Solder Contact Angle Results

We measured the solder angle measurements with a computer-aided program. Thanks to this program, we were able to see how many degrees of contact angle the solder made with the surface. According to these results, the solder paste without epoxy addition has the largest solder angle. This solder angle value was found to be 29. According to the literature, this is a very good solder angle value. It is possible to say that the lower the solder angle value, the better the solder is. Because the lower the solder angle, the larger the spreading area. From this we can understand that these two values are opposite to each other. The soldering contact angle of Sn-58Bi solder paste with 1 wt.% epoxy is 23. The soldering contact angle value of Sn-58Bi solder paste with 3 wt.% epoxy is 18. The soldering contact angle of Sn-58Bi solder paste with 5 wt.% epoxy is 13. The soldering angle value of Sn-58Bi solder paste with 7 wt.% epoxy is 21. The soldering contact angle value of Sn-58Bi solder paste with 9 wt.% epoxy is 18. However, there is a difference in soldering angles on the right and left sides equally in the product, so this was not a desirable feature. According to these results, the addition of epoxy caused a decrease in the solder angle up to a certain level. However, as the amount of epoxy added increased, the solder angle increased. In order to verify the accuracy of the results obtained and that the same results were obtained each time, 5 trials were performed for each sample. The results were very close in all trials. According to the results, the Sn-Bi solder with the best solder angle was the solder added with 5 wt.% epoxy. We can find the solder angles in Figure 3.7.

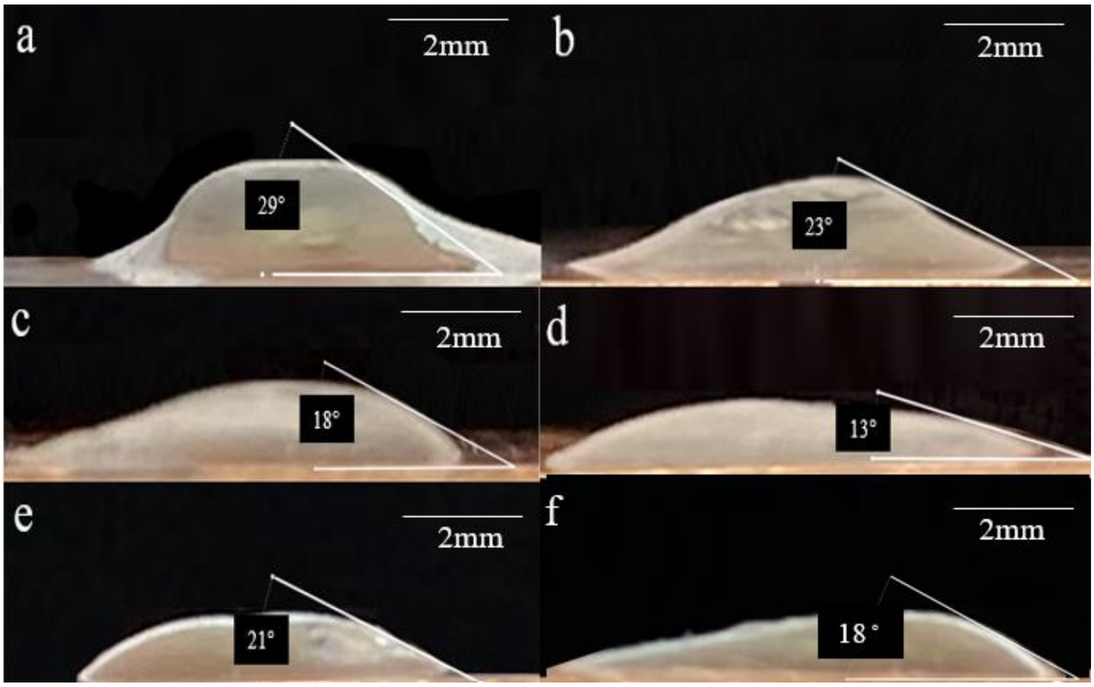

Figure 3.7 Solder contact angle, (a) Epoxy-free Sn-Bi solder, (b) Sn-58Bi solder containing 1 wt.% epoxy, (c) Sn-58Bi solder containing 3 wt.% epoxy, (d) Sn-58Bi solder containing 5 wt.% epoxy, (e) Sn-58Bi solder containing 7 wt.% epoxy, (f) Sn-58Bi solder containing 9 wt.% epoxy

It was seen that the soldering property improves when epoxy was added to Sn-Bi solder paste at the ideal ratio. With the amount of epoxy added, the outer wall of the surface was covered with epoxy and acts as a protective barrier.

3.6 Solder Spreading Area Results

The spreading area of the solder is proportional to the angle the solder makes with the surface. The smaller the angle at which the solder was soldered, the larger the area over which it can spread. The test was repeated 5 times for each sample. The results were very similar. When the spreading area calculations were made, it was seen that the solder with the best spreading area was the solder containing 5 wt.% epoxy.

Compared to the epoxy-free Sn-Bi solder, the solder containing 5 wt.% epoxy had 2.8 times more spreading area. This shows that the most ideal solder is Sn-Bi solder paste with 5 wt.% epoxy content. Excessive addition of epoxy also affects the soldering properties of Sn-Bi solder paste. Because thermoset epoxy retains the applied heat on its surface. When the amount of epoxy increases, the epoxy on the surface thickens at that rate. When the epoxy thickens, the heat conduction value decreases. Because polymers have poor thermal conductivity. When this thick layer was high, the soldering of the solder is badly affected. We can see the prepared samples in Figure 3.8.

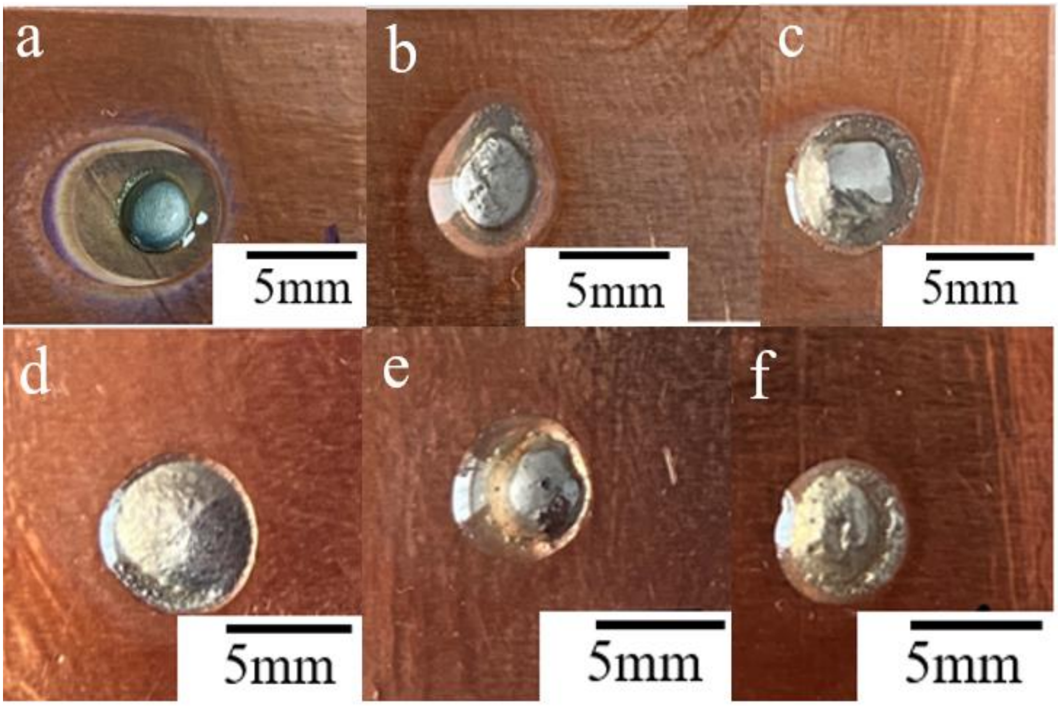

Figure 3.8 Solder spreading area, (a) Epoxy-free Sn-Bi solder, (b) Sn-58Bi solder containing 1 wt.% epoxy, (c) Sn-58Bi solder containing 3 wt.% epoxy, (d) Sn-58Bi solder containing 5 wt.% epoxy, (e) Sn-58Bi solder containing 7 wt.% epoxy, (f) Sn-58Bi solder containing 9 wt.% epoxy

As seen in figure d, the solder with the best spreading range is the solder with 5% epoxy content. Looking carefully at figure e, we cannot say that the solder is a uniform solder because of the epoxy. So, it is very important to add the right amount of epoxy. A graph of the spreading area and soldering angle are shown in Figure 3.9.

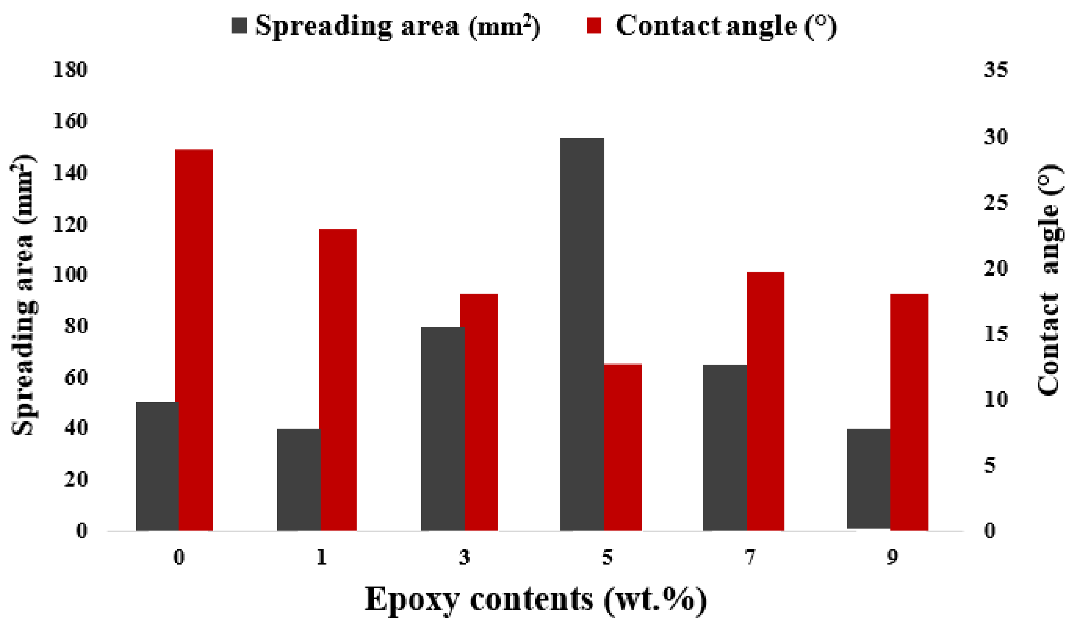

Figure 3.9 Spreading area and contact angle curves of Sn-58Bi solder paste for different epoxy resin contents

3.7 Drop Test Results for Sn-Bi Solders

In the drop test, an oscillation occurs as a result of the drop and this oscillation is what destroys the structure of the solder. There was a noticeable difference in the specimens subjected to the drop test. The test was repeated 5 times for each sample. The drop test results were obtained based on the average of the results. The drop test results are as follows. Sn-58Bi solder without epoxy lost its solder function after 820 drops. Sn-58Bi solder with epoxy content of 1 wt.% lost its solder function after 865 drops. Sn-58Bi solder with epoxy content of 3 wt.% lost its solder function after 1311 drops. Sn-58Bi solder with epoxy content of 5 wt.% lost its solder function after 2124 drops. Sn-58Bi solder with epoxy content of 7 wt.% lost its solder function after 2932 drops. Sn-58Bi solder with epoxy content of 9 wt.% lost its solder function after 3340 drops. As a result of these results, the epoxy-free solder paste exhibited the lowest performance. The solder with 5 wt.% content, which we consider ideal, performed 2.6 times better than the epoxy-free solder. Although solders with higher epoxy content perform better against drop, the best one is Sn-58Bi with 5 wt.% content in all conditions, considering the other properties. The graph of the drop test result can be seen in Figure 3.10.

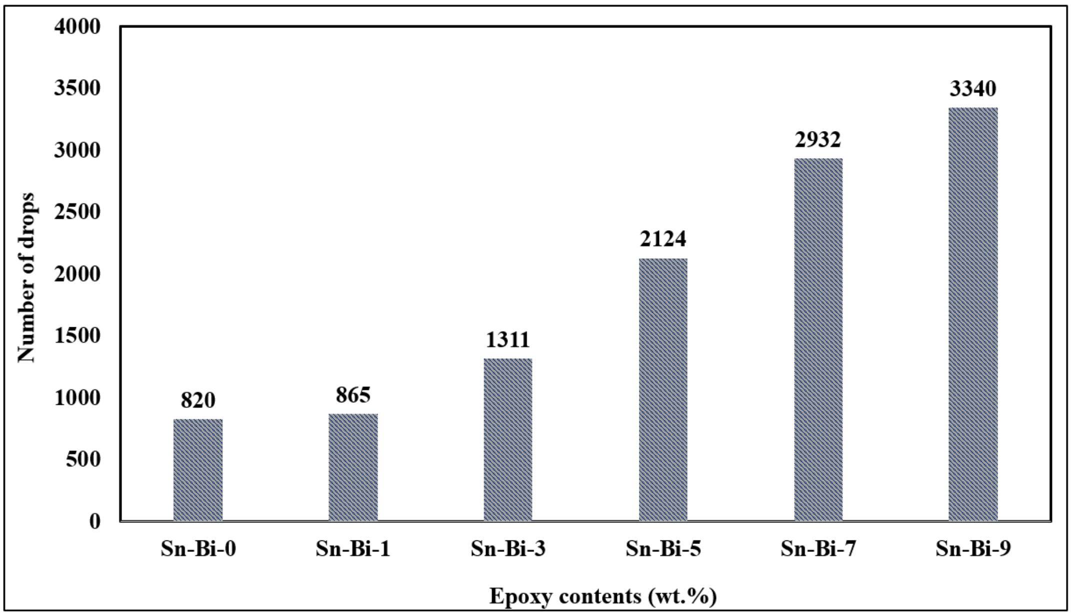

Figure 3.10 Shows the drop test results

3.8 Differential Scanning Calorimeter (DSC) Results

First, we looked at the DSC graph of our Sn-58Bi solder paste to find out at what temperature it melted. The solder paste we used melted at 139.1 °C, in line with the literature. The DSC graph gives us the most accurate information about how many degrees the Sn-58Bi solder will melt. 10 °C/min heating was preferred as the DSC operating temperature. We can see the DSC graph of Sn-58Bi solder paste in Figure 3.11.

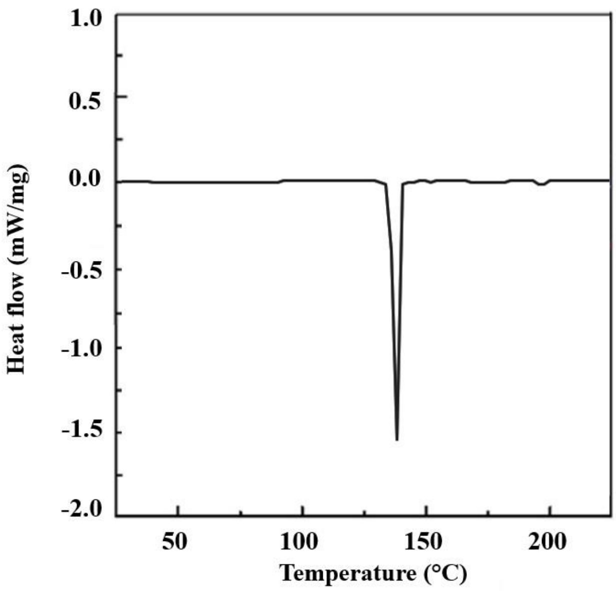

Figure 3.11 DSC curve of the eutectic Sn-58Bi alloy

In epoxy polymers, the results generally seen in DSC analysis are glass transition temperature and melting temperature. Since the polymer we use is in liquid form, it is very difficult to see the glass transition temperature. Therefore, a temperature above the glass transition temperature was preferred. 100 °C was preferred as the starting temperature. For the same polymer, 5 °C/min and 10 °C/min heating was preferred as DSC operating temperature. As a result of DSC obtained with 5 °C/min heating, the curing peak temperature was measured as 142.3 °C. As a result of DSC obtained with 10 °C/min heating, the curing peak temperature was measured as 153.2 °C. The curing of epoxy resin is an exothermic process. We can see the DSC graph of the epoxy used in Figure 3.12.

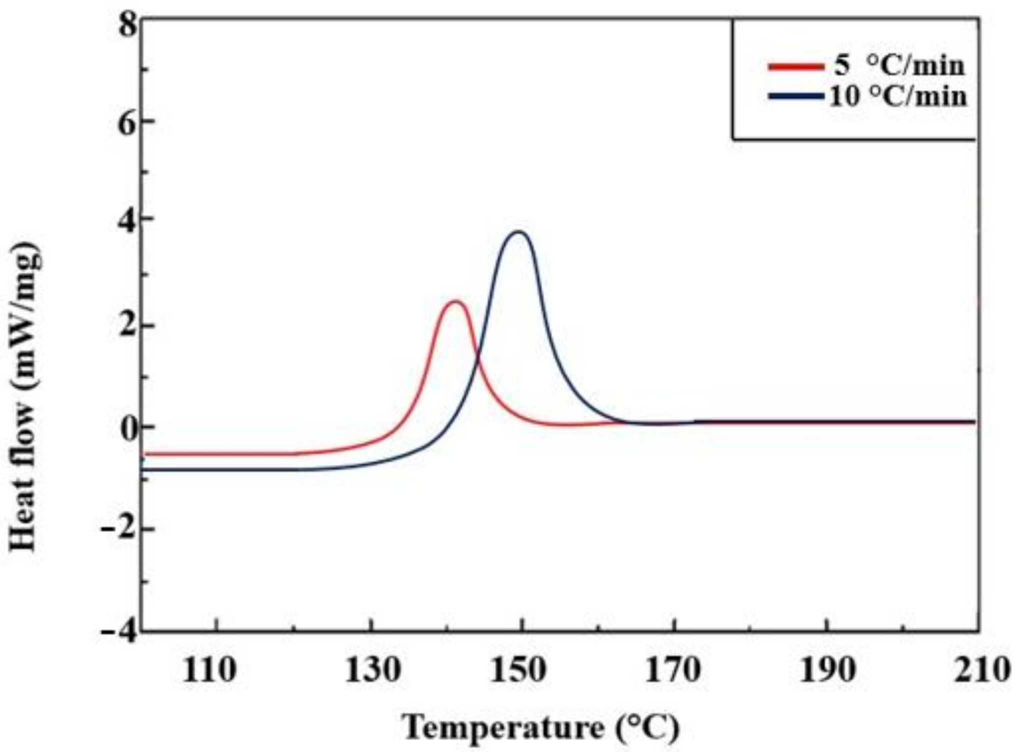

Figure 3.12 The thermoset epoxy DSC curves at different heating rates

3.9 Scanning Electron Microscope (SEM) Results

3.9.1 SEM Images of Sn-58Bi Solder Pastes Exposed to Sun

We can see SEM images of samples exposed to the sun in Figure 3.13. When taking SEM images of the samples, 3000X magnification was used.

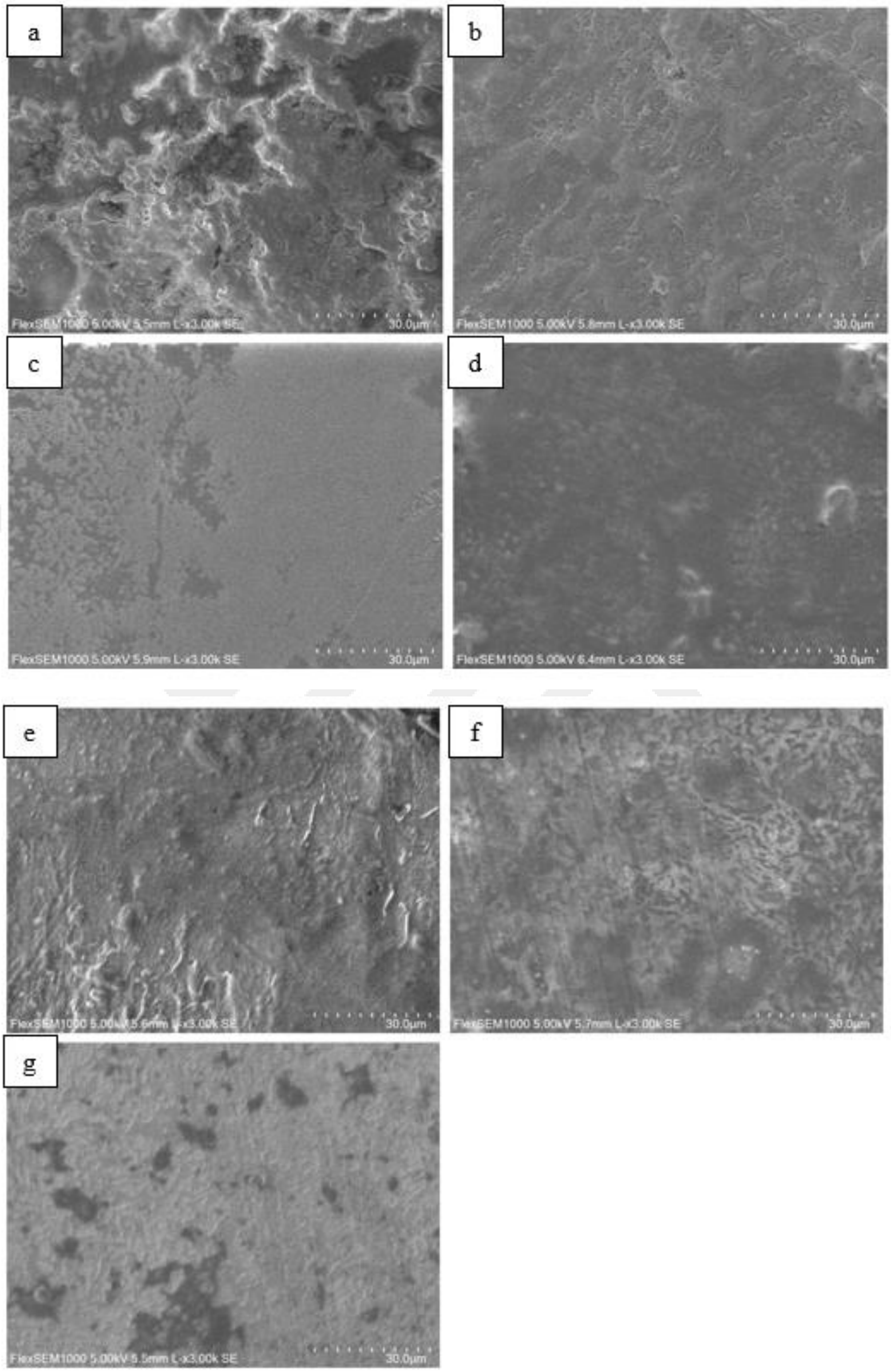

Figure 3.13 SEM images of Sn-58Bi Solder Pastes Exposed to Sun, (a) Epoxy-free Sn-Bi solder, (b) Sn-58Bi solder containing 1 wt.% epoxy, (c) Sn-58Bi solder containing 3 wt.% epoxy, (d) Sn-58Bi solder containing 5 wt.% epoxy, (e) Sn-58Bi solder containing 7 wt.% epoxy, (f) Sn-58Bi solder containing 9 wt.% epoxy, (g) epoxy and flux-free Sn-Bi solder, 3k magnification

3.9.2 SEM Images of Sn-58Bi Solder Kept in an Oven at 100 °C for 3 Days

We can see SEM images of Sn-58Bi solder kept in an oven at 100 °C for 3 days in Figure 3.14. When taking SEM images of the samples, 3000X magnification was used.

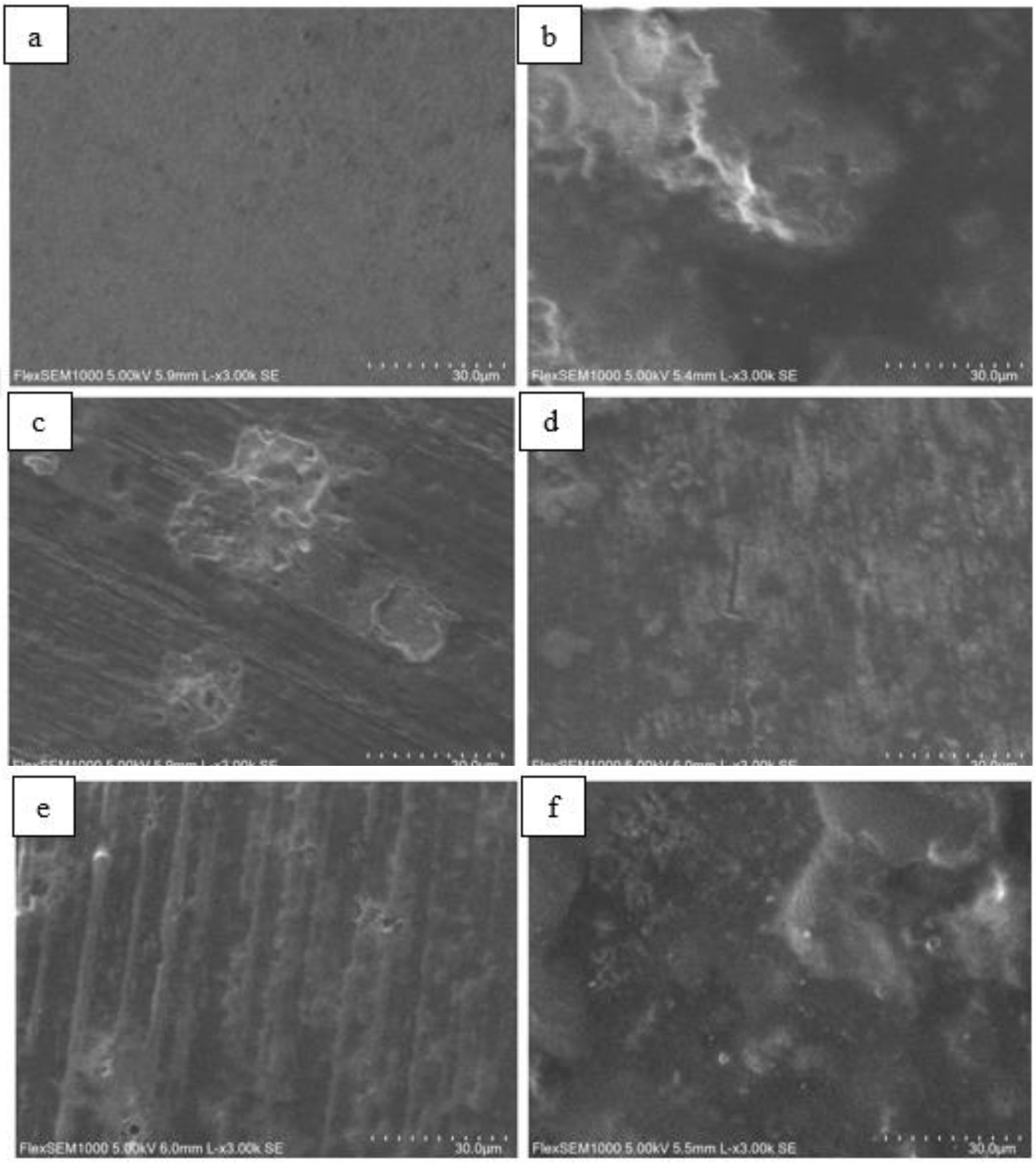

Figure 3.14 SEM images of Sn-58Bi solder kept in an oven at 100 °C for 3 days, (a) Epoxy-free Sn-Bi solder, (b) Sn-58Bi solder containing 1 wt.% epoxy, (c) Sn-58Bi solder containing 3 wt.% epoxy, (d) Sn-58Bi solder containing 5 wt.% epoxy, (e) Sn-58Bi solder containing 7 wt.% epoxy, (f) Sn-58Bi solder containing 9 wt.% epoxy, 3k magnification

3.9.3 SEM Images of Sn-58Bi Solder

We can see SEM images of Sn-58Bi solder in Figure 3.15. When taking SEM images of the samples, 3000X magnification was used.

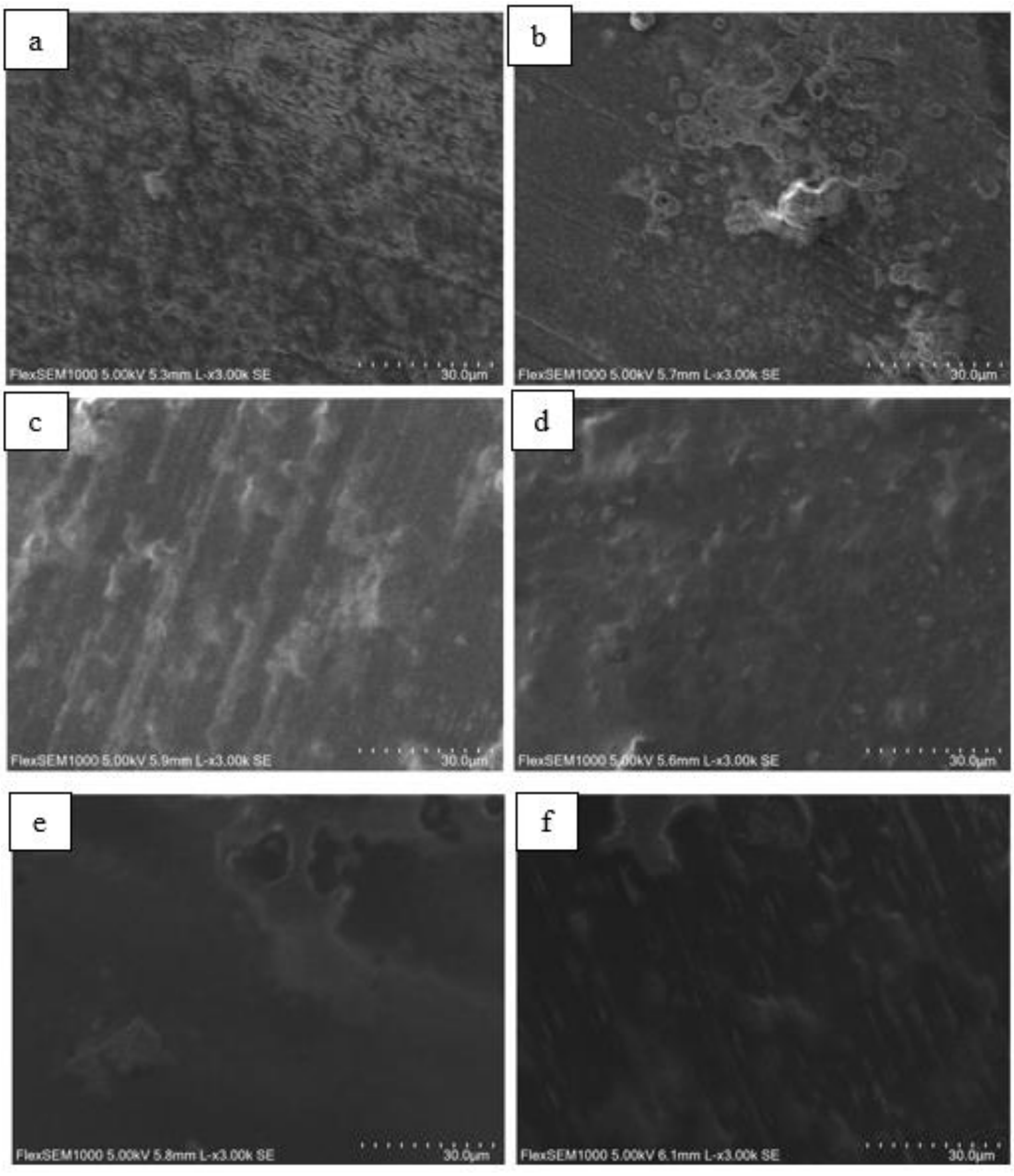

Figure 3.15 SEM images of Sn-58Bi solder, (a) Epoxy-free Sn-Bi solder, (b) Sn-58Bi solder containing 1 wt.% epoxy, (c) Sn-58Bi solder containing 3 wt.% epoxy, (d) Sn-58Bi solder containing 5 wt.% epoxy, (e) Sn-58Bi solder containing 7 wt.% epoxy, (f) Sn-58Bi solder containing 9 wt.% epoxy, 3k magnification

3.9.4 SEM Images of Sn-58Bi Solder Subjected to Thermal Cycling Testing

We can see SEM images of Sn-58Bi solder subjected to Thermal Cycling Testing in Figure 3.16. When taking SEM images of the samples, 3000X magnification was used.

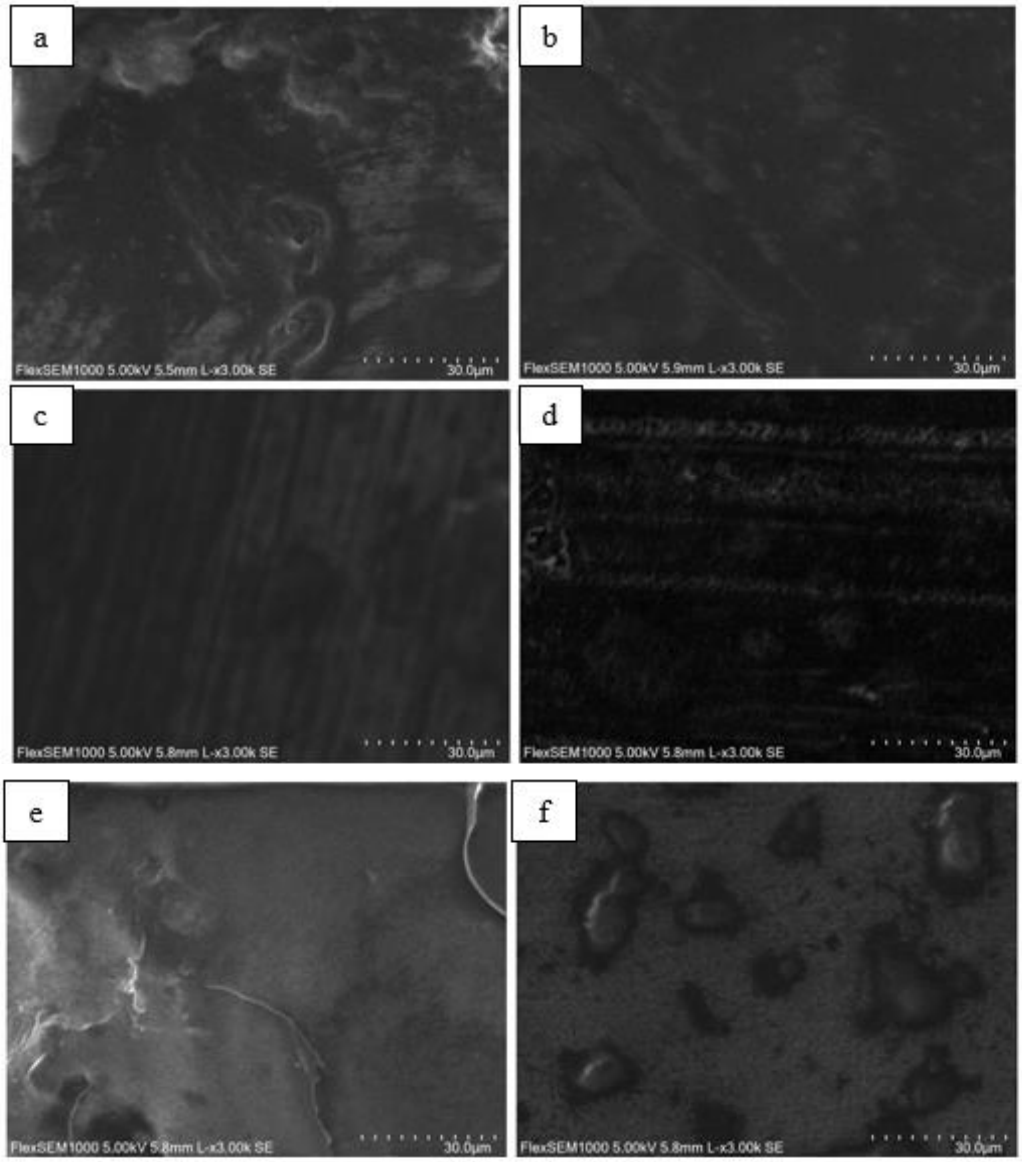

Figure 3.16 SEM images of Sn-58Bi solder subjected to Thermal Cycling Testing, (a) Epoxy-free Sn-Bi solder, (b) Sn-58Bi solder containing 1 wt.% epoxy, (c) Sn-58Bi solder containing 3 wt.% epoxy, (d) Sn-58Bi solder containing 5 wt.% epoxy, (e) Sn-58Bi solder containing 7 wt.% epoxy, (f) Sn-58Bi solder containing 9 wt.% epoxy, 3k magnification

3.9.5 SEM Images of Single-step and Double-step Sn-58Bi Soldering

We can see SEM images of single-step and double-step Sn-58Bi soldering in Figure 3.17. When taking SEM images of the samples, 3000X magnification was used.

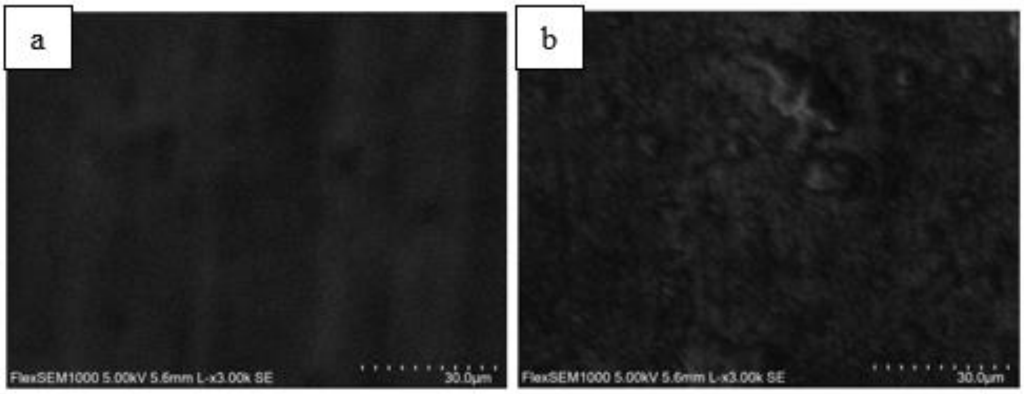

Figure 3.17 SEM images of single-step and double-step Sn-58Bi soldering, (a) single soldering process of epoxy-free Sn-58Bi solder, (b) double soldering process of epoxy-free Sn-58Bi solder, 3k magnification

As a result of SEM images, it is possible to say that epoxy added Sn-58Bi solders are generally better protected in terms of microstructure. Because there is an outer wall that protects the structure against external factors. This outer wall is a strong structure that protects the product against moisture, oxidation and chemical corrosion. Therefore, if the epoxy addition is sufficient enough to cover the surface of the solder, our solder is protected. It is possible to say that this protective layer is present in solder where the epoxy addition is 5wt.%. As a result of higher epoxy addition, pits were observed on the surface of the solder. This will prevent the solder from exhibiting the desired properties.

SEM images, the biggest reason why some samples could not be imaged is due to very etching. The other reason is that the metallography process is difficult because our sample is a soft metal product. The softness of the solder obtained made this process difficult and it was difficult to get clear images in some products. In SEM images, bright area was Bi and black area was Sn. Because the etching material used interacted with the Sn surface.

3.10 Hardness Results

It is possible to say that the hardness values were in line with our expectations. In the solder kept in the sun, epoxy-added solder gave better results in terms of hardness. The hardness difference between them is between 2-4 HV. In the samples kept in the oven for 3 days at 100 °C, the hardness values were very close to each other. The biggest reason for this is that the heat is evenly distributed to all samples after a certain period of time. The sample subjected to the re-soldering process showed a hardness difference of 1 HV in terms of hardness. The hardness of all specimens decreased as a result of the thermal cycling test. The main reason for this is due to prolonged exposure to heat and cold air. The hardness value of epoxy added solders was 1HV higher. The test was repeated 5 times for each sample. The results of the hardness values were obtained based on the average of the results. From this we can draw the following conclusion. The added epoxy has a positive effect on the hardness of the solder. Because Sn-58Bi maintains the hardness value of the solder. The table of hardnesses is given in Table 3.1.

Table 3.1 Hardness results

Sample Number	Solder paste content	Epoxy content by weight	Hardness Value (HV) (245.2 mN)	Treatment
1	Sn-58Bi	0%	28.2	Sun exposure
2	Sn-58Bi	1%	30.0	Sun exposure
3	Sn-58Bi	3%	29.4	Sun exposure
4	Sn-58Bi	5%	30.3	Sun exposure
5	Sn-58Bi	7%	31.0	Sun exposure
6	Sn-58Bi	9%	31.9	Sun exposure
7	Sn-58Bi	0%	27.0	Sun exposure
8	Sn-58Bi	0%	26.5	100 °C oven for 3 days
9	Sn-58Bi	1%	26.5	100 °C oven for 3 days
10	Sn-58Bi	3%	26.7	100 °C oven for 3 days
11	Sn-58Bi	5%	26.9	100 °C oven for 3 days
12	Sn-58Bi	7%	27.1	100 °C oven for 3 days
13	Sn-58Bi	9%	27.0	100 °C oven for 3 days
14	Sn-58Bi	0%	27.9	Only soldered
15	Sn-58Bi	1%	27.8	Only soldered
16	Sn-58Bi	3%	27.9	Only soldered
17	Sn-58Bi	5%	28.2	Only soldered
18	Sn-58Bi	7%	28.1	Only soldered
19	Sn-58Bi	9%	28.2	Only soldered
20	Sn-58Bi	0%	28.0	One step soldering
21	Sn-58Bi	0%	29.0	Double step soldering
22	Sn-58Bi	0%	20.8	Thermal Cycling
23	Sn-58Bi	1%	21.0	Thermal Cycling
24	Sn-58Bi	3%	21.2	Thermal Cycling
25	Sn-58Bi	5%	21.6	Thermal Cycling
26	Sn-58Bi	7%	22.2	Thermal Cycling
27	Sn-58Bi	9%	22.3	Thermal Cycling

CHAPTER 4

CONCLUSION

In this thesis, thermoset epoxy was added into Sn-58Bi solder. Thanks to the added epoxy, the brittle structure of Bismuth was eliminated. This gives us a more reliable solder structure. DSC, SEM, hardness measurement was used for characterization. Another important parameter is the contact angle. Solder angles were characterized and it was subjected to drop test.

In the first part of the study, a 20-38 µm grain size powder alloy containing eutectic 42Sn58Bi was mixed with flux to produce a solder paste with the best results. The flux added was 11.5 wt.%. After this step, the Sn-58Bi solder paste was mixed with thermoset epoxy. With this mixture, we obtained a composite structure. The product with the best properties in this composite structure was solder with 5 wt.% thermoset epoxies.

The results obtained from the DSC analysis determined our roadmap. It showed that our Sn-58Bi solder melted at 139.1 °C. It also gave us the curing temperature of the polymer used, allowing us to obtain our samples at low temperatures. Thus, the increasing energy need in the world will reduce the energy need to some extent by using low temperature solder pastes. It has a suitable contact angle for surface soldering and offers the possibility of layered soldering by choosing solder with more than one melting temperature on the same electronic board. Otherwise, desoldering all components at the same time may cause problems in production.

According to the solder contact angle results, thermosetting epoxy adding reduces the solder angle. Solder angle has a very important place in solder paste. Because the lower the solder angle, the higher the spreading area. This parameter is one of the most important factors determining the life of the solder. Our composite structure with the best solder angle was Sn-58Bi with 5 wt.% epoxy content. This solder angle reduced the solder angle by more than half compared to Sn-58Bi solder without epoxy addition.

According to the drop test, there was a big difference between the solder without epoxy addition and the solder with epoxy addition. The main reason for this difference is that epoxy prevents the formation and progression of cracks on the surface of the solder. In addition, thanks to the high adhesion properties of epoxy, it can adhere more firmly to the surfaces. Thanks to this feature, it will offer the possibility of soldering to different surfaces, not only soldering between metals. In the drop test, the solder with 5 wt.% content, which we consider ideal, performed 2.6 times better than the epoxy-free solder.

SEM analysis, changes in the structures of Sn and Bi metals in the structure of Sn-58Bi solder due to the addition of epoxy could be observed. As a result of this observation, it can be concluded that there was growth in the structures without epoxy addition and less growth in the added solder. Since the growth of the Bi phase is the biggest factor that will cause the structure to be brittle, the addition of epoxy acts as a preventive function against this brittleness. It is thought that the structure will maintain its form as long as it is not exposed to high heat treatment. After the soldering process, as long as the Sn-58Bi solder does not exceed 70 °C, there is no formation in the structure that will affect the solder. However, epoxy-free solder is adversely affected when it exceeds 70 °C and waits for a long time after soldering. Since the epoxy used is a type of epoxy that can withstand 90 °C continuously, it can be easily used in many places where solder is used.

The epoxy addition used in the study creates a protective layer on the solder. Since this layer prevents the solder from being directly exposed to water and moisture, the negative effect of these factors on the solder is eliminated. Electronic circuits used in structures sent into space are exposed to humidity due to the large temperature change. Since moisture will cause these circuits to oxidize and short-circuit, the circuits must be protected against this effect. This can be avoided if epoxy added solder is preferred. In drop tests, it was observed that solder made with epoxy addition was much more durable than normal solder, so it is thought that epoxy added solder will protect the solder against vibration. It will also protect the solder against sudden temperature changes as epoxy has a bad heat conduction.

As a result, the obtained Sn-58Bi composite solder with thermosetting epoxy resin has great advantages. Since it allows soldering at low temperatures, it does not damage the components around it. Most importantly, the epoxy allows the solder to be soldered on different surfaces. In this way, it will be easier to develop different compositions and create different products. The Sn-58Bi composite solder paste with 5% epoxy content by weight we obtained was the product that gave the best result as a result of these trials. Since the outer side of this product is epoxy, it is not affected by water and moisture. It acts as a protective barrier against oxidation or other external factors. The biggest feature that distinguishes it from other epoxy structures is that it has a flexible structure. Thanks to this flexible structure, there are no scratches on the surface.

REFERENCES

[1] Jiang, N. et al. Reliability issues of lead-free solder joints in electronic devices. Sci. Technol. Adv. Mater. 20, 876–901. 2019

[2] Schwaneke, A.E.; Falke, W.L.; Miller, V.R. Surface tension and density of liquid tin-lead solder alloys. J. Chem. Eng. Data, 23, 298–301. 1978

[3] Gan, K.; Ngan, A. The unusual size effect of eutectic Sn/Pb alloys in the micro regime: Experiments and modeling. Acta Mater., 151, 282–292. 2018

[4] Siewart, T.; Liu, S.; Smith, D.R.; Madeni, J.C. Database for Solder Properties with Emphasis on New Lead-free Solders. In Properties of Lead-Free Solders; National Institute of Standards: Gaithersburg, MD, USA, 2002.

[5] Kang, S. K., Lauro, P. A., Shih, D. Y., Henderson, D. W. & Puttlitz, K. J. Microstructure and mechanical properties of lead-free solders and solder joints used in microelectronic applications. IBM J. Res. Dev. 49, 607–620. 2005

[6] Olofinjana, A.; Haque, R.; Mathir, M.; Voo, N. Studies of the solidification characteristics in Sn-Ag-Cu-Bi solder alloys. Procedia Manuf., 30, 596–603. 2019

[7] Zhong, S. juan, Zhang, L., Li, M. lan, Long, W. min & Wang, F. jiang. Development of lead-free interconnection materials in electronic industry during the past decades: Structure and properties. Mater. Des. 215, 110439. 2022

[8] Kang, H., Rajendran, S. H. & Jung, J. P. Low melting temperature sn-bi solder: Effect of alloying and nanoparticle addition on the microstructural, thermal, interfacial bonding, and mechanical characteristics. Metals (Basel). 11, 1–25. 2021

[9] Yim, B.-S.; Youn, H.J.; Lee, J.I.; Kim, J.-M. Influence of Carbon Nanotube Concentration on the Interconnection Properties of Solderable Isotropic and Anisotropic Conductive Adhesive. J. Weld. Join., 38, 152–157. 2020

[10] Huang, Y.C.; Chen, S.W. Effects of Co alloying and size on solidification and interfacial reactions in Sne57 wt.%Bie(Co)/Cu couples. J. Electron. Mater., 40, 62–70. 2011

[11] Ren, G.; Wilding, I.J.; Collins, M.N. Alloying influences on low melt temperature SnZn and SnBi solderalloys for electronic interconnections. J. Alloys Compd., 665, 251–260. 2016

[12] Choi, J.Y.; Park, D.; Oh, T.S. Chip Interconnection Process for Smart Fabrics Using Flip-chip Bonding of SnBi Solder. J. Microelectron. Packag. Soc., 19, 71–76. 2012

[13] Torres, A.; Hernández, L.; Domínguez, O. Effect of Antimony Additions on Corrosion and Mechanical Properties of Sn-Bi Eutectic Lead-Free Solder Alloy. Mater. Sci. Appl., 3, 355–362. 2012

[14] Singh, A.; Durairaj, R. Study on Hardness and Shear Strength with Microstructure Properties of Sn52Bi/Cu + 1% Al2O3 Nanoparticles. IOP Conf. Ser. Mater. Sci. Eng., 834, 1–5. 2020

[15] Zhou, S.; Yang, C.-H.; Lin, S.-K.; AlHazaa, A.N.; Mokhtari, O.; Liu, X.; Nishikawa, H. Effects of Ti addition on the microstructure, mechanical properties and electrical resistivity of eutectic Sn58Bi alloy. Mater. Sci. Eng. A, 744, 560–569. 2019

[16] Miao, H.W.; Duh, J.G. Microstructure evolution in Sn-Bi and Sn-Bi-Cu solder joints under thermal aging. Mater. Chem. Phys., 71, 255–271. 2001

[17] McCluskey, P.; Munamarty, R.; Pecht, M. Popcorning in PBGA Packages During IR Reflow Soldering. Microelectron. Int., 14, 20–23. 1997

[18] Shen, J.; Pu, Y.; Yin, H.; Luo, D.; Chen, J. Effects of minor Cu and Zn additions on the thermal, microstructure and tensile properties of Sn–Bi-based solder alloys. J. Alloys Compd., 614, 63–70. 2014

[19] Dušek, K. et al. Understanding the Effect of Reflow Profile on the Metallurgical Properties of Tin–Bismuth Solders. Metals (Basel). 12. 2022

[20] Anam, A., Gamit, N., Prajapati, V. & Dholakiya, B. Z. An overview of kaolin and its potential application in thermosetting polymers. Mater. Today Commun. 36, 106827. 2023

[21] S.J. Park, F.L. Jin, L. Nicolais, in: L. Nicolais, A. Borzacchiello (Eds.), Wiley Encyclopedia of Composites, John Wiley & Sons. 2011

[22] Park, S. J., Kim, M. H., Lee, J. R. & Choi, S. Effect of fiber-polymer interactions on fracture toughness behavior of carbon fiber-reinforced epoxy matrix composites. J. Colloid Interface Sci. 228, 287–291. 2000

[23] Jiang, W., Jin, F. L. & Park, S. J. Thermo-mechanical behaviors of epoxy resins reinforced with nano-Al 2O 3 particles. J. Ind. Eng. Chem. 18, 594–596. 2012

[24] Mousavifard, S. M., Nouri, P. M. M., Attar, M. M. & Ramezanzadeh, B. The effects of zinc aluminum phosphate (ZPA) and zinc aluminum polyphosphate (ZAPP) mixtures on corrosion inhibition performance of epoxy/polyamide coating. J. Ind. Eng. Chem. 19, 1031–1039. 2013

[25] Jin, F. L., Ma, C. J. & Park, S. J. Thermal and mechanical interfacial properties of epoxy composites based on functionalized carbon nanotubes. Mater. Sci. Eng. A 528, 8517–8522. 2011

[26] Erukhimovich, I. & de la Cruz, M. O. Phase equilibria and charge fractionation in polydisperse polyelectrolyte solutions. 3348–3356. 2004

[27] Zhang, W., Li, X. & Yang, R. Pyrolysis and fire behaviour of epoxy resin composites based on a phosphorus-containing polyhedral oligomeric silsesquioxane (DOPO-POSS). Polym. Degrad. Stab. 96, 1821–1832. 2011

[28] Rochester, J. R. Bisphenol A and human health: A review of the literature. Reprod. Toxicol. 42, 132–155. 2013

[29] Vogel, S. A. The politics of plastics: the making and unmaking of bisphenol a 'safety'. Am. J. Public Health 99 Suppl 3, 559–566. 2009

[30] Delfosse, V. et al. Structural and mechanistic insights into bisphenols action provide guidelines for risk assessment and discovery of bisphenol A substitutes. Proc. Natl. Acad. Sci. U. S. A. 109, 14930–14935. 2012

[31] Jindal, S., Maka, V. K. & Moorthy, J. N. Selective sensing of aliphatic biogenic polyamines by a zwitterionic Cd-MOF based on bisimidazole tetracarboxylic acid linker. J. Mater. Chem. C 8, 11449–11456. 2020

[32] Wan, J., Li, C., Fan, H. & Li, B. G. Branched 1,6-Diaminohexane-Derived Aliphatic Polyamine as Curing Agent for Epoxy: Isothermal Cure, Network Structure, and Mechanical Properties. Ind. Eng. Chem. Res. 56, 4938–4948. 2017

[33] Van Der Pol, T. P. A. et al. The Mechanism of Dedoping PEDOT:PSS by Aliphatic Polyamines. J. Phys. Chem. C 123, 24328–24337. 2019

[34] Kadoya, W. M. et al. Covalent bonding of aromatic amine daughter products of 2,4-dinitroanisole (DNAN) with model quinone compounds representing humus via nucleophilic addition. Environ. Pollut. 268, 115862. 2021

[35] Cheng, A. Di, Zong, M. H., Lu, G. H. & Li, N. Solvent-Promoted Oxidation of Aromatic Alcohols/Aldehydes to Carboxylic Acids by a Laccase-TEMPO System: Efficient Access to 2,5-Furandicarboxylic Acid and 5-Methyl-2-Pyrazinecarboxylic Acid. Adv. Sustain. Syst. 5, 1–8. 2021

[36] Garcia, J. M., R.B. Bernardino, I., Calasans, V. & Giudici, R. Kinetics of the hydrolysis of acetic anhydride using reaction calorimetry: effects of strong acid catalyst and salts. Chem. Eng. Res. Des. 166, 29–39. 2021

[37] Zhang, X. et al. Direct synthesis of quinazolinones via the carbon-supported acid-catalyzed cascade reaction of isatoic anhydrides with amides and aldehydes. Tetrahedron Lett. 66, 152835. 2021

[38] Wang, F., Huang, Y., Zhang, Z. & Yan, C. Interfacial reaction and mechanical properties of Sn-Bi solder joints. Materials (Basel). 10. 2017

[39] Gain, A. K. & Zhang, L. Growth mechanism of intermetallic compound and mechanical properties of nickel (Ni) nanoparticle doped low melting temperature tin–bismuth (Sn–Bi) solder. J. Mater. Sci. Mater. Electron. 27, 781–794. 2016

[40] Miao, H. W. & Duh, J. G. Microstructure evolution in Sn-Bi and Sn-Bi-Cu solder joints under thermal aging. Mater. Chem. Phys. 71, 255–271. 2001

[41] Liu, Y. et al. Microstructure and mechanical properties of as-reflowed Sn58Bi composite solder pastes. J. Mater. Process. Technol. 238, 290–296. 2016

[42] Kang, H., Rajendran, S. H. & Jung, J. P. Low melting temperature sn-bi solder: Effect of alloying and nanoparticle addition on the microstructural, thermal, interfacial bonding, and mechanical characteristics. Metals (Basel). 11, 1–25. 2021

[43] WANG, F., LV, Z., Sun, L., CHEN, H. & LI, M. Microstructure changes in Sn-Bi solder joints reinforced with Zn@Sn particles in thermal cycling and thermomigration. J. Taiwan Inst. Chem. Eng. 146, 104871. 2023

[44] Yang, L., Du, C., Dai, J., Zhang, N. & Jing, Y. Effect of nanosized graphite on properties of Sn-Bi solder. J. Mater. Sci. Mater. Electron. 24, 4180–4185. 2013

[45] Li, X. guang, Yang, X. jun, He, D. yong & Ma, L. Study on the properties of epoxy-based Sn–58Bi solder joints. Microelectron. Reliab. 148, 115144. 2023

[46] Yang, L. et al. Influence of BaTiO3 Nanoparticle Addition on Microstructure and Mechanical Properties of Sn-58Bi Solder. J. Electron. Mater. 44, 2473–2478. 2015

[47] Zhang, C., Liu, S. D., Qian, G. T., Zhou, J. & Xue, F. Effect of Sb content on properties of Sn - Bi solders. Trans. Nonferrous Met. Soc. China (English Ed. 24, 184–191. 2014

[48] Tan, M. Y. et al. Dynamic wetting behavior and solder ball spattering formation of Sn-Bi solder pastes during reflow soldering process. 2016 17th Int. Conf. Electron. Packag. Technol. ICEPT 2016 974–978. 2016

[49] Guo, F. et al. Resistance changes in eutectic Sn-Bi solder joints during electromigration. J. Electron. Mater. 38, 2756–2761. 2009

[50] Tan, X. F. et al. The Effect of Temperature on the Electrical Resistivity of Sn-Bi Alloys. J. Electron. Mater. 53, 1183–1191. 2024

[51] Kattner, U. R. Phase diagrams for lead-free solder alloys. Jom 54, 45–51. 2002

[52] Satyanarayan, K.N. Prabhu, Wetting behavior and interfacial microstructure of Sn–Ag–Zn solder alloys on nickel coated aluminum substrates, Mater. Sci. Technol. 27,1157–1162. 2011

[53] S.F. Wang, T. Yang, S.C. Lee, Wettability of electrode metals on barium titanate substrate, J. Mater. Sci. 36, 825–829. 2001

[54] L. Sun, M.H. Chen, L. Zhang, L.S. Xie, Effect of addition of CuZnAl particle on the properties of Sn solder joint, J. Mater. Process. Technol. 278, 116507. 2019

[55] R.K. Kaushik, U. Batra, J.D. Sharma, Structural, thermal and wetting characteristics of novel low Bi-low Ag containing Sn–x. Ag–0.7Cu–1.0Bi (x=0.5 to 1.5) alloys for electronic application, Met. Mater. - Int, 1–14. 2020

[56] Z. Moser, W. Ga˛ sior, J. Pstrus´, A. De˛bski, Wettability studies of Pb-Free soldering materials, Int. J. Theosophy’s. 29, 1974–1986. 2008

[57] L.K. Zang, Z.F. Yuan, H.Y. Xu, B.S Xu, Wetting process and interfacial characteristic of Sn–3.0Ag–0.5Cu on different substrates at temperatures ranging from 503 K to 673 K, Appl. Surf. Sci. 257, 4877–4884. 2011

[58] T.T. Kyaw, P. Tunthawiroon, K. Kanlayasiri, K. Yamanaka, A. Chiba, A study on wettability and formation of intermetallic phase between Co-Cr-Mo alloy and Sn-Solder used as a potential under bump metallization for flip-chip packages, Intermetallics 125, 106875. 2020

[59] X. Chen, F. Xue, J. Zhou, Y. Yao, Effect of In on microstructure, thermodynamic characteristic and mechanical properties of Sn-Bi based lead-free solder, J. Alloys Compd. 633, 377–383. 2015

[60] W. Yang, Z. Yang, Y. Fu, A. Yu, Y. Zhan, Effect of graphene nanosheet addition on the wettability and mechanical properties of Sn-20Bi-xGNS/Cu solder joints, Materials 13, 3968. 2020

[61] J. Fan, H. Zhai, Z. Liu, X. Wang, Y. Li, H. Gao, J. Liu, Effect of Ni content on the microstructure formation and properties of Sn-0.7Cu-xNi solder alloys, J. Mater. Eng. Perform. 29, 4934–4943. 2020

[62] L. Zhang, J. Han, F. Liu, Y. Guo, C. He, Effect of nano-particles TiO2 on the microstructures and properties of SnAgCu solders, Rare Metal Mat. Eng. 42, 1897–1900. 2013

[63] Steinmann, W., Walter, S., Beckers, M., Seide, G. & Gries, T. Thermal Analysis of Phase Transitions and Crystallization in Polymeric Fibers. Appl. Calorim. a Wide Context - Differ. Scanning Calorimetry, Isothermal Titration Calorim. Microcalorim. 2013

[64] Weilie, Z., Robert, A., Lin, W. Z. and David, J. Scanning Microscopy for Nanotechnology, Springer,1-40. 2006

[65] Implementation of 3000-watt inverter. Jurnal Polimesin. Polimesin 20, 121–127. 2023